Electronic Supplementary Information

Quenched Skeletal Ni as the effective catalyst for selective partial hydrogenation of polycyclic aromatic hydrocarbons

Chengyun Liu , Zeming Rong*, Zhuohua Sun, Yong Wang, Wenqiang Du, Yue Wang and Lianhai Lu
State Key Laboratory of Fine Chemicals, Dalian University of Technology, Dalian 116024, China
Corresponding author Tel.: +86 411 84986242;
E-mail address: *zeming@dlut.edu.cn*

Contents:

1. Preparation and characterization of Quenched Skeletal Ni

The rapidly Quenched Skeletal Ni catalyst (QS Ni) was prepared as following procedures: At first, Ni-Al-Mo mother alloy was prepared by melting 46.4 wt% Ni, 49.3 wt% Al and 4.3 wt% Mo at 1800 K for at least 30 min with vigorous stirring. And then, Ni-Al-Mo metallic liquid was rapid quenched on a fast-rotating copper roller to form alloy ribbon. After ball-milling and sieving, the powder fraction of 150-300 mesh was collected and then the Al was leached out by using excess amount of 17 wt% NaOH aqueous solution at 373.15 K for 3 hours. The prepared Quenched Skeletal Ni was kept in water to keep from the deactivation by air.

The surface morphology and structural characteristics of the QS Ni were characterized by X-ray diffraction (XRD) pattern which was collected on a Rigaku D/MAX2400 diffractometer with Cu Ka (40 kV, 100 mA) radiation. Scanning electron microscopy (SEM) was measured by Philips XL 30 and before being transferred into the SEM chamber the QS Ni was washed by ethanol and dispersed on the sample holder and then quickly moved into the vacuum evaporator (LDM-150D) in which a thin gold film was deposited after drying in vacuum. Specific surface area measurements were obtained by volumetric nitrogen adsorption using a Micromeritics ASAP-2010 instrument. Measurements were obtained using 0.10 g of catalyst weighed into a sample tube and conditioned at 250 ^{o}C for 4 h and 5×10^{-5} Torr. Following out-gassing, the samples were cooled to ambient temperature prior to adsorption measurements. The analysis was carried out by dosing nitrogen at -196 ^{o}C, with the variation in pressure allowing the adsorbed volume of N_2 to be determined.

2. Experimental procedures

The catalytic hydrogenation reaction was typically conducted in a stainless-steel autoclave reactor heated in oil bath. For each run, a predetermined quantity of reactant and THF solvent was placed into the reactor (70 mL capacity) together with an appropriate amount of catalyst. After the reactor was sealed, it was purged by flushing with 1.0 MPa of N_2 for three times and then H_2 for three times. When the autoclave was heated to a required temperature, it was pressurized with H_2 at the selected setting point. The reaction time was reckoned when the agitation started from this point. A constant pressure was maintained throughout the reaction period. Samples taken at regular intervals were analyzed by GC.

3. Quantum calculations of molecular configuration

A quantum mechanical approach, in particular the hybrid Density Functional B3LYP method with a split valence basis set and d polarisation functions 6-31G(d) was used for molecular models of PAHs. The calculations performed using Gaussian 03 software.

This computational model is a reasonable compromise between accuracy and computational cost for isolated systems energy calculations.

4. Analytical and characterization data

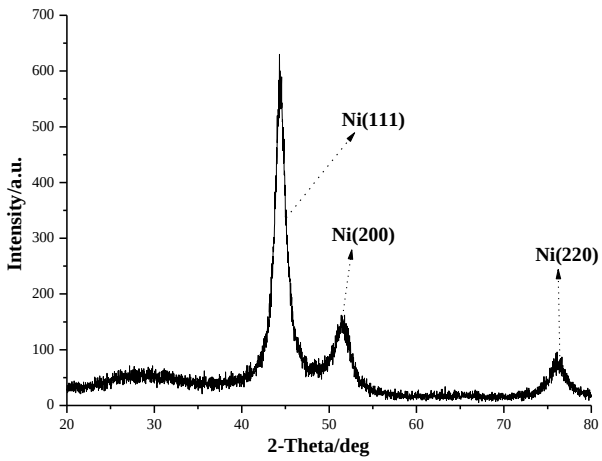

Fig. S1 XRD patterns of quenched skeletal Ni

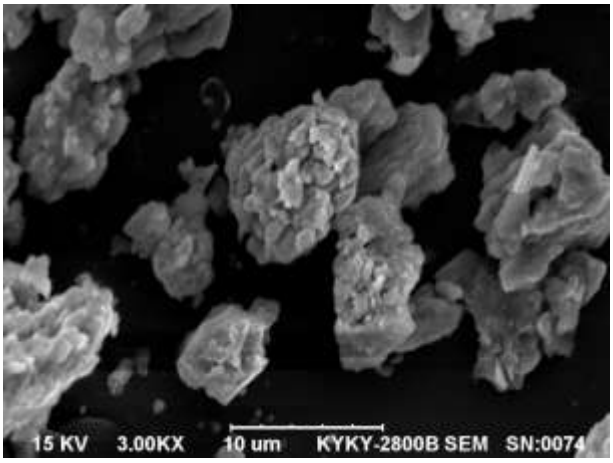

Fig. S2 SEM image of QS Ni

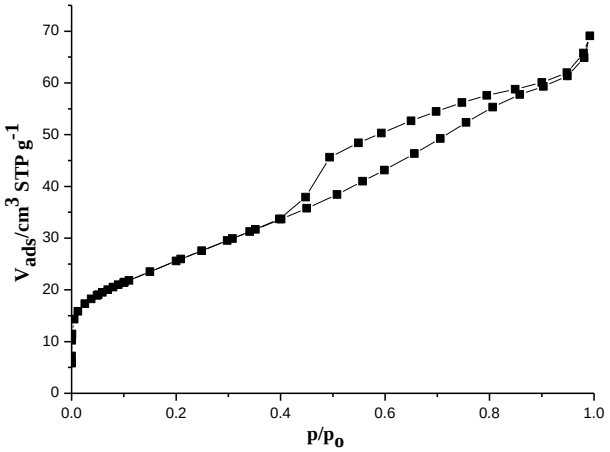

Fig. S3 Nitrogen isotherms at 77 K for QS Ni

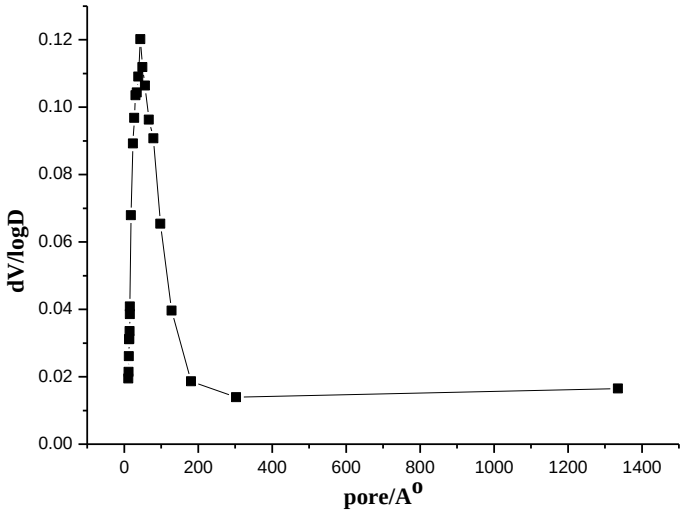

Fig. S4 Pore-size distribution of QS Ni

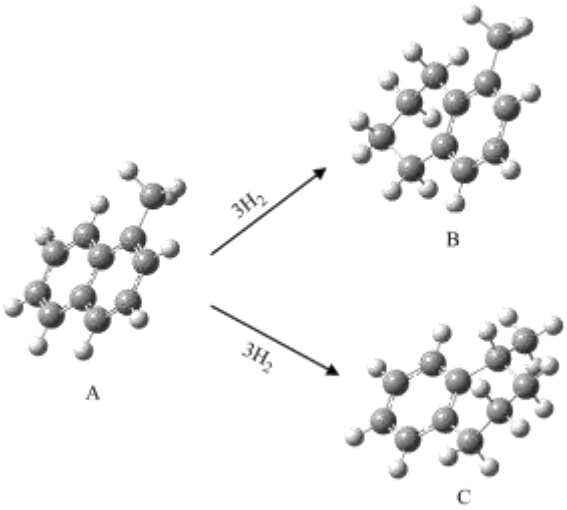

Fig. S5 Transformations of molecular structure during the hydrogenation process of 1-methylnaphthalene

A: 1-methylnaphthalene; B: 5-methyl-1,2,3,4-tetrahydronaphthalene; C: 1-methyl-1,2,3,4-tetrahydronaphthalene

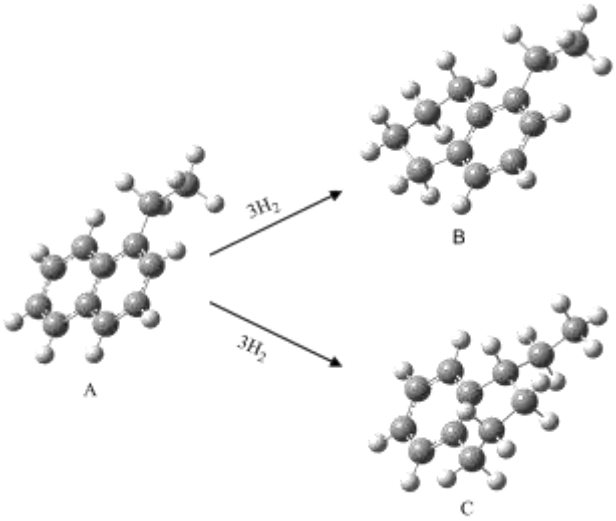

Fig. S6 Transformations of molecular structure during the hydrogenation process of 1-ethylnaphthalene

A: 1-ethylnaphthalene; B: 5-ethyl-1,2,3,4-tetrahydronaphthalene; C: 1-ethyl-1,2,3,4-tetrahydronaphthalene

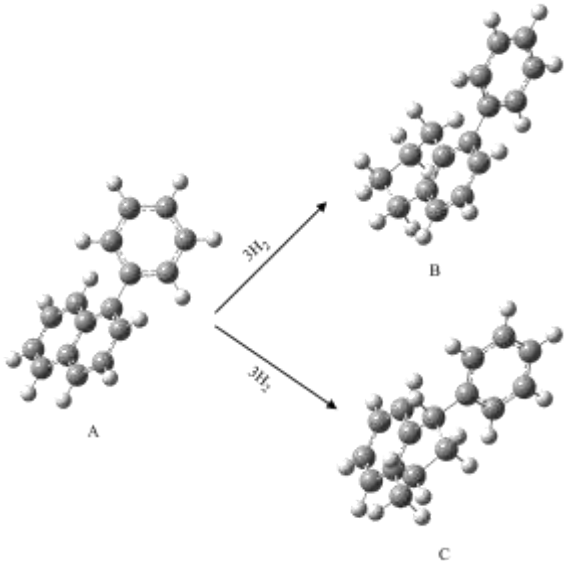

Fig. S7 Transformations of molecular structure during the hydrogenation process of 1-phenylnaphthalene

A: 1-phenylnaphthalene; B: 5-phenyl-1,2,3,4-tetrahydronaphthalene; C: 1-phenyl-1,2,3,4-tetrahydronaphthalene

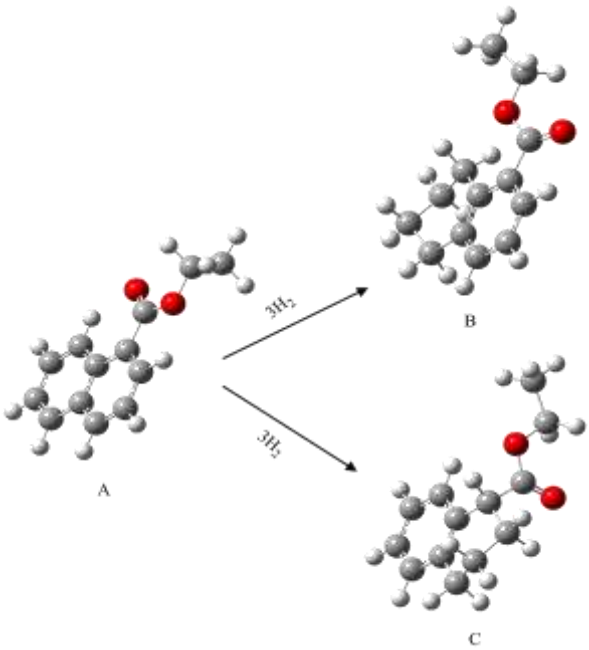

Fig. S8 Transformations of molecular structure during the hydrogenation process of ethyl 1-naphthoate

A: ethyl 1-naphthoate; B: ethyl 5,6,7,8-tetrahydronaphthalene-1-carboxylate; C: ethyl 1,2,3,4-tetrahydronaphthalene-1-carboxylate

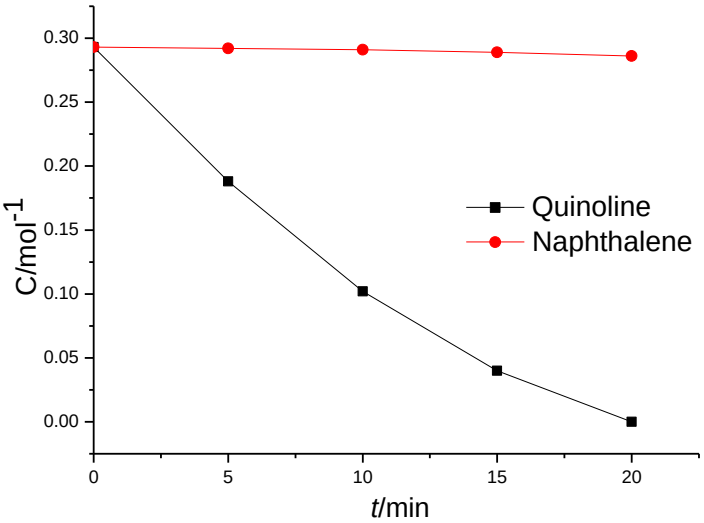

Fig. S9 Concentration-time plots for the hydrogenation of naphthalene and quinoline in the same catalytic system

Reaction conditions: 373 K, 1.5 MPa, 5.9 mmol naphthalene and 5.9 mmol quinoline，20 mL THF, 0.2 g QS Ni.

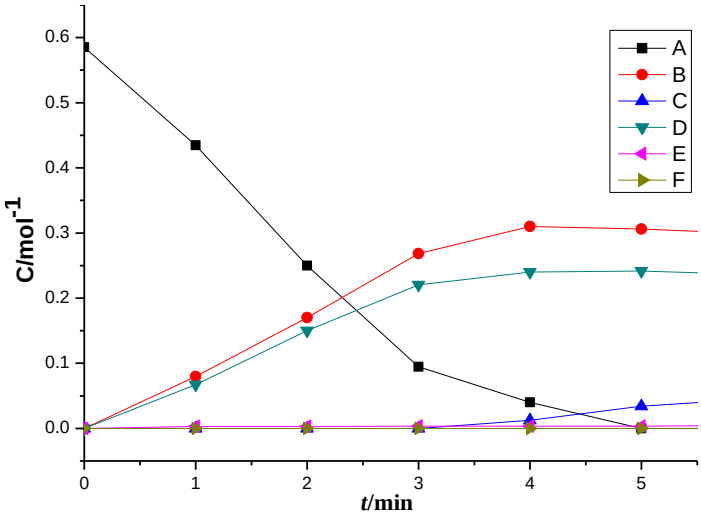

(a)

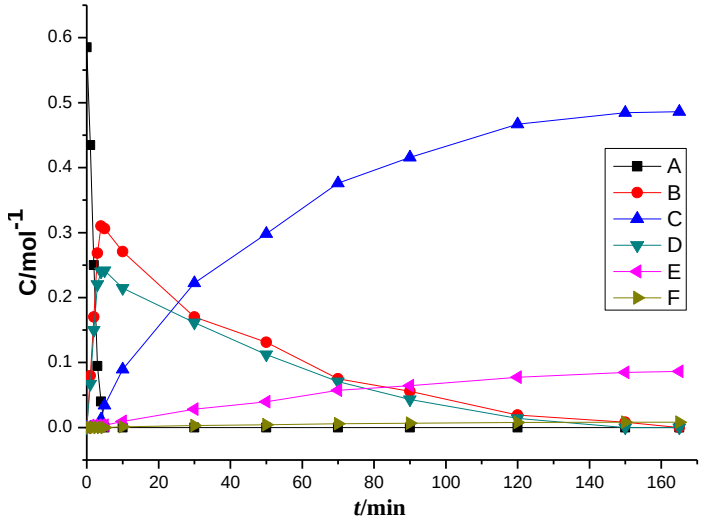

(b)

Fig. S10 The concentration-time plots for the selective hydrogenation of anthracene over QS Ni (a) the first stage of the reaction; (b) the whole stage of the reaction

A: anthracene; B: 1,2,3,4-tetrahydroanthracene; C: 1,2,3,4,5,6,7,8-octahydroanthracene; D: 9,10-dihydroanthracene; E: 1,2,3,4,4a,9,9a,10-octahydroanthracene; F: tetradecahydroanthracene

Reaction conditions: 373.15 K, 1.5 MPa, 11.7 mmol substrates, 20 mL THF, 0.2 g QS Ni.

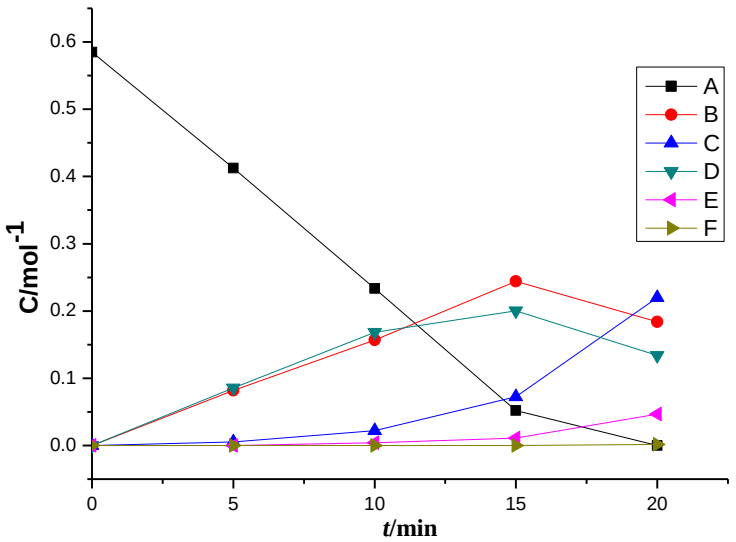

(a)

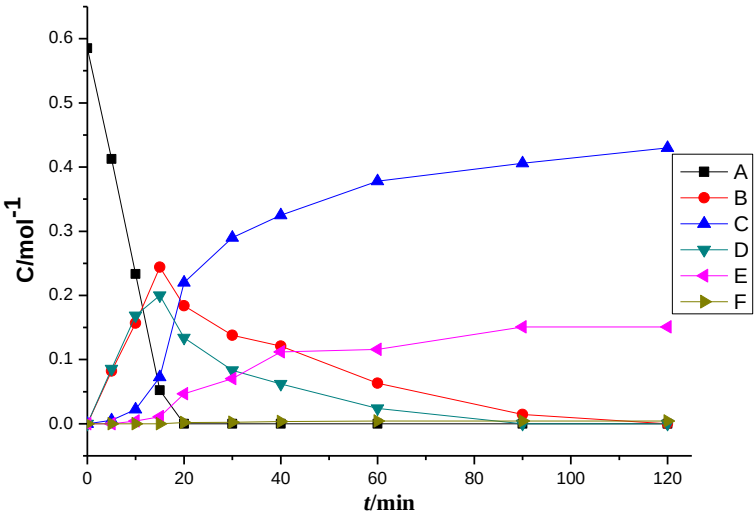

(b)

Fig. S11 The concentration-time plots for the selective hydrogenation of phenanthrene over QS Ni (a) the first stage of the reaction; (b) the whole stage of the reaction

A: phenanthrene; B: 1,2,3,4-tetrahydrophenanthrene; C: 1,2,3,4,5,6,7,8-octahydrophenanthrene; D: 9,10-dihydrophenanthrene; E: 1,2,3,4,4a,9,10,10a-octahydrophenanthrene; F: peryhydrophenanthrene

Reaction conditions: 373.15 K, 1.5 MPa, 11.7 mmol substrates, 20 mL THF, 0.2 g QS Ni.

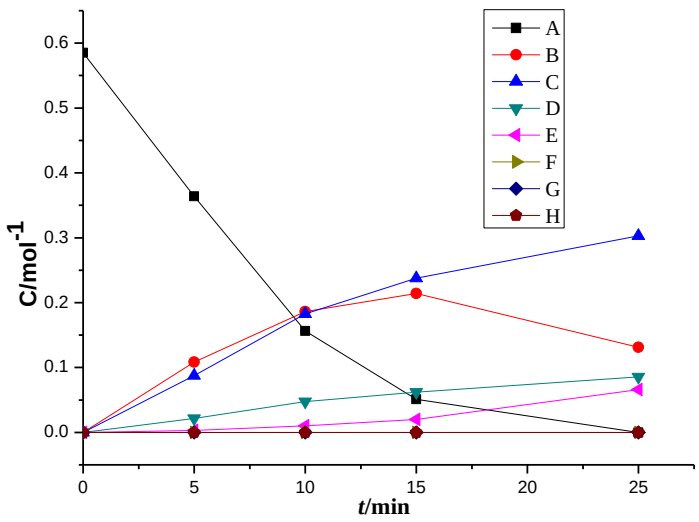

(a)

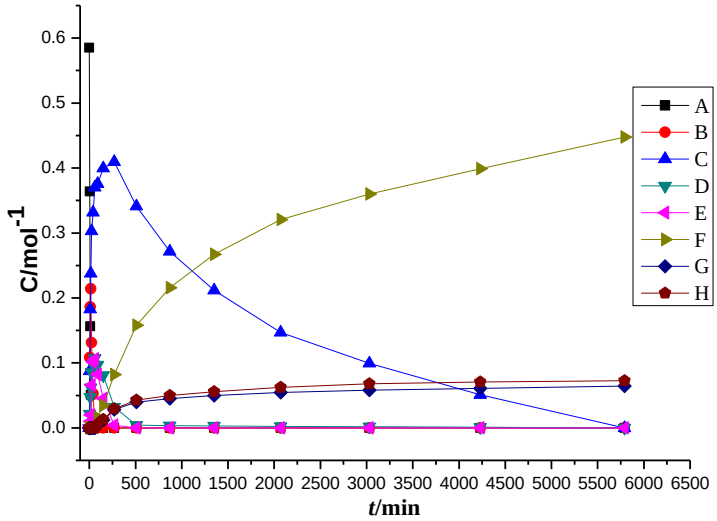

(b)

Fig. S12 The concentration-time plots for the selective hydrogenation of pyrene over QS Ni (a) the first stage of the reaction; (b) the whole stage of the reaction

A: pyrene; B: 4,5-dihydropyrene; C: 1,2,3,6,7,8-hexahydropyrene; D: 1,2,3,3a,4,5-hexahydropyrene; E: 4,5,9,10-tetrahydropyrene; F: 1,2,3,3a,4,5,5a,6,7,8-octahydropyrene; G: 1,2,3,3a,3a1,4,5,9,10,10a-octahydropyrene; H: hexadecahydropyrene

Reaction conditions: 373.15 K, 1.5 MPa, 11.7 mmol substrates, 20 mL THF, 0.2 g QS Ni.

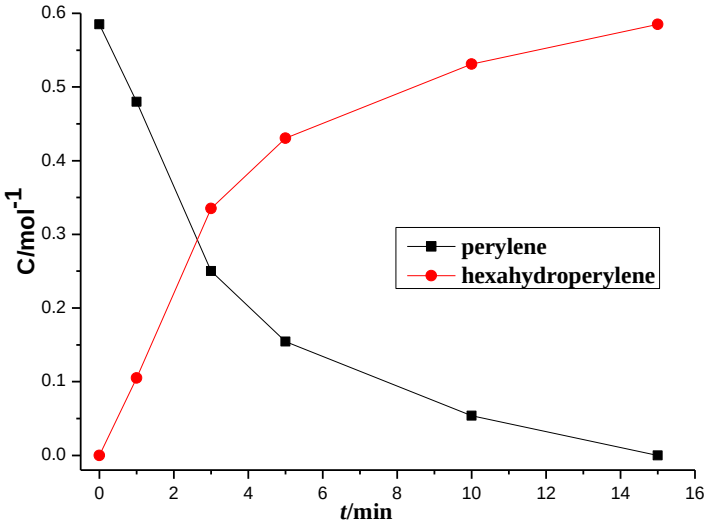

(a)

The concentration-time plots for the first stage of hydrogenation of perylene

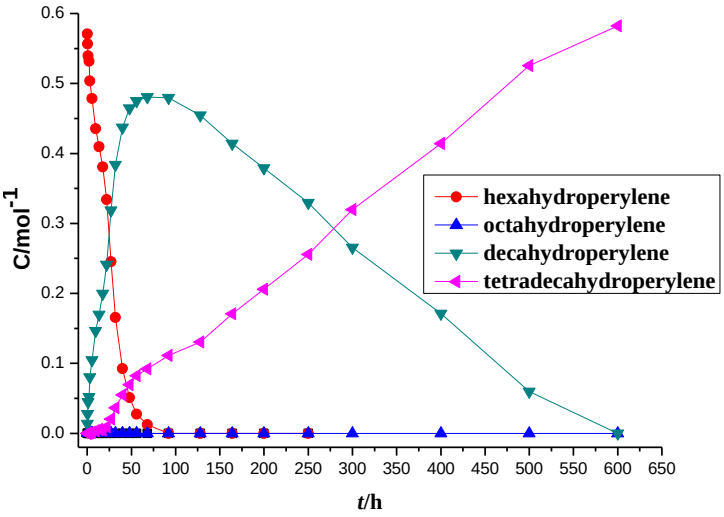

(b)

Fig. S13 The concentration-time plots of hydrogenation of perylene over QS Ni

(a) the first stage of the reaction; (b) the second stage of the reaction

Reaction conditions: 373.15 K, 1.5 MPa, 11.7 mmol substrates, 20 mL THF, 0.2 g QS Ni.

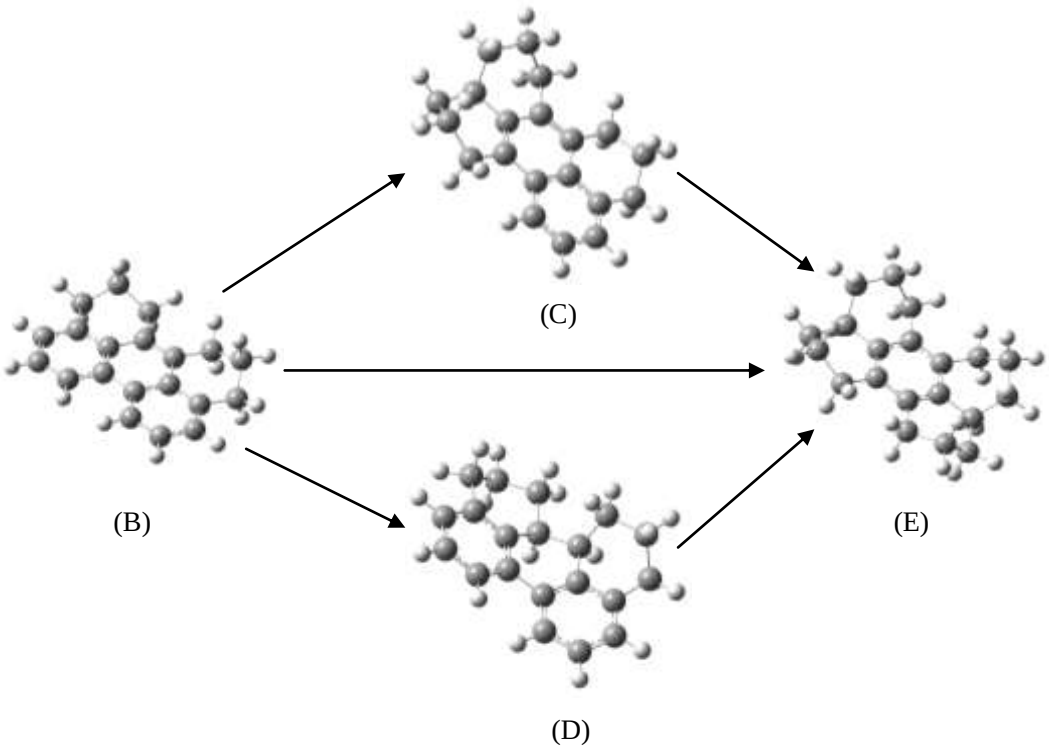

Fig. S14 Transformation of molecular configurations during the hydrogenation process of perylene (B) 1,2,3,10,11,12-H_6perylene; (C) 1,2,3,3a,4,5,6,7,8,9-H_{10}perylene; (D) 1,2,3,10,11,12,12a,12b-H_8perylene; (E) 1,2,3,3a,4,5,6,7,8,9,9a,10,11,12-H_{14}perylene

The molecular configurations were simulated by hybrid Density Functional B3LYP method with a split valence basis set and d polarisation functions 6-31G(d) over Gaussian 03 software.

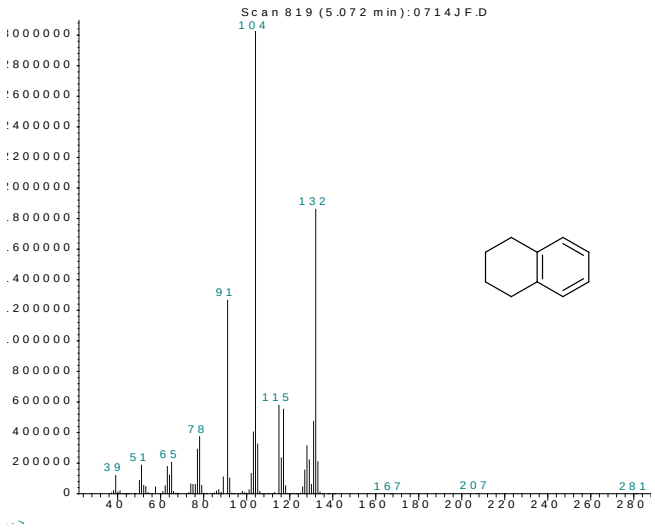

Fig. S15 Mass spectra of tetralin

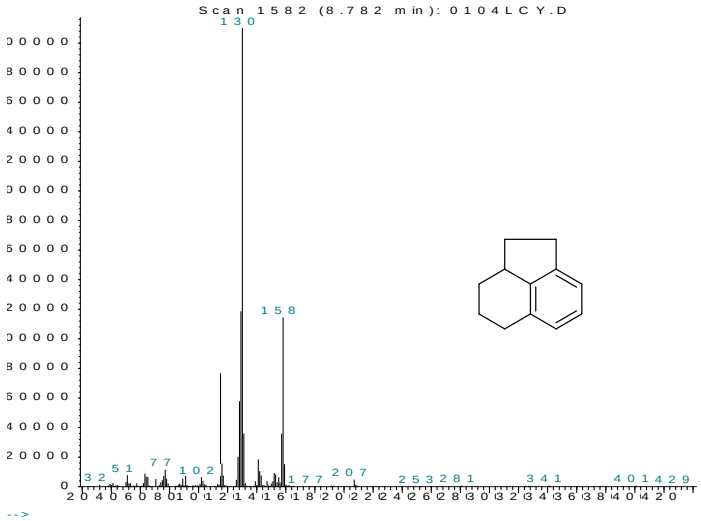

Fig. S16 Mass spectra of 1,2,2a,3,4,5-hexahydroacenaphthylene

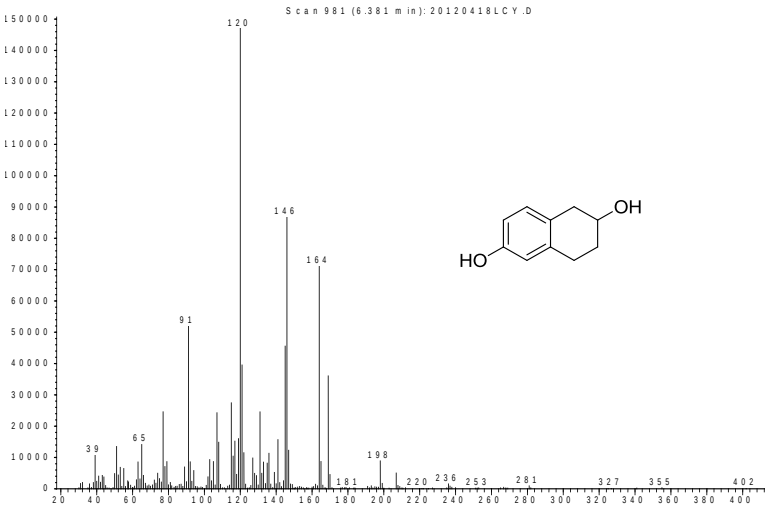

Fig. S17 Mass spectra of 1,2,3,4-tetrahydronaphthalene-2,6-diol

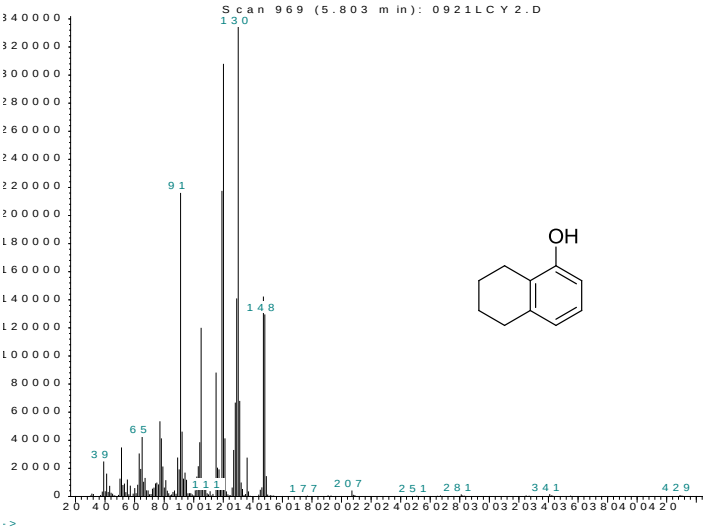

Fig. S18 Mass spectra of 1,2,3,4-tetrahydronaphthalen-1-ol

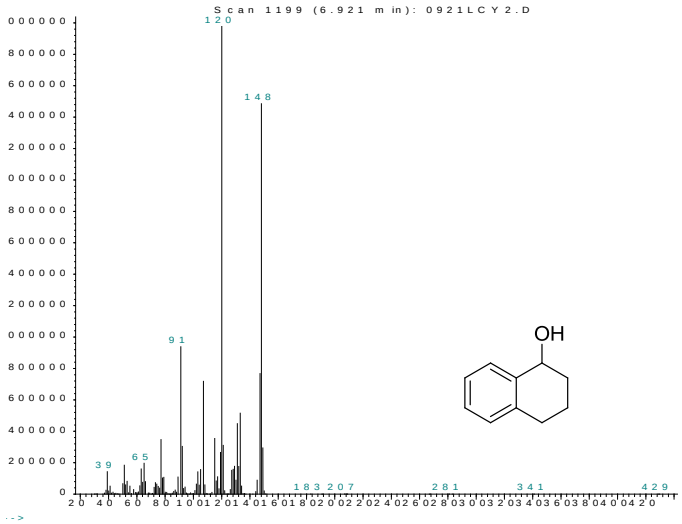

Fig. S19 Mass of 5,6,7,8-tetrahydronaphthalen-1-ol

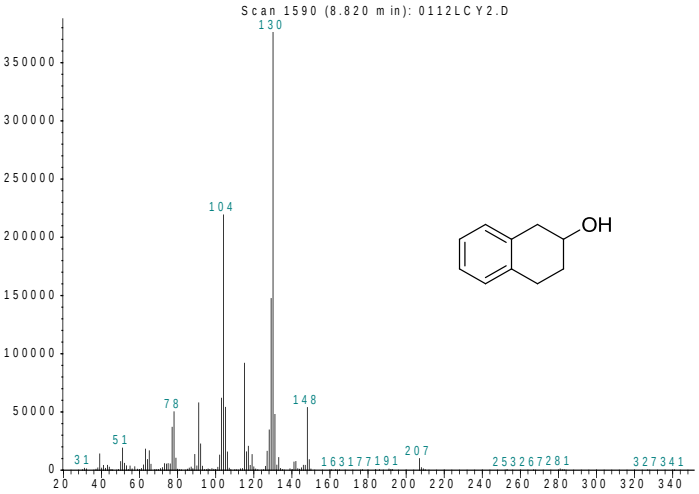

Fig. S20 Mass spectra of 1,2,3,4-tetrahydronaphthalen-2-ol

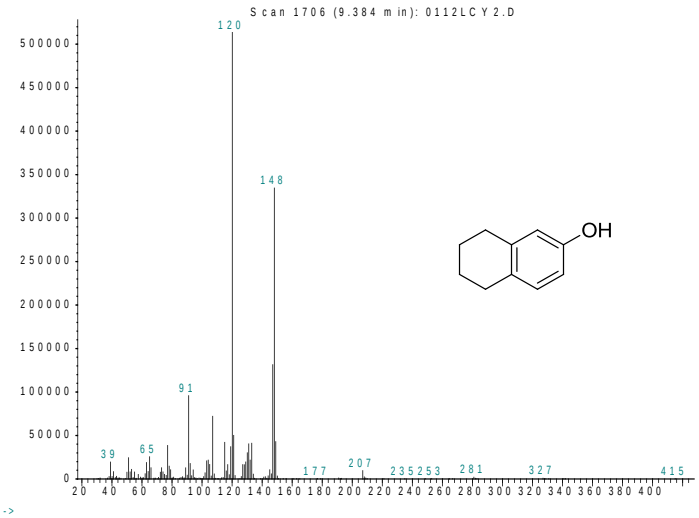

Fig. S21 Mass spectra of 5,6,7,8-tetrahydronaphthalen-2-ol

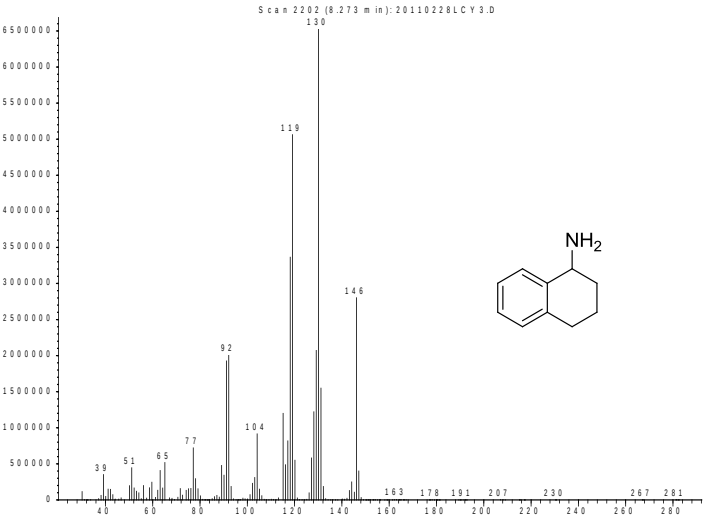

Fig. S22 Mass spectra of 1,2,3,4-tetrahydronaphthalen-1-amine

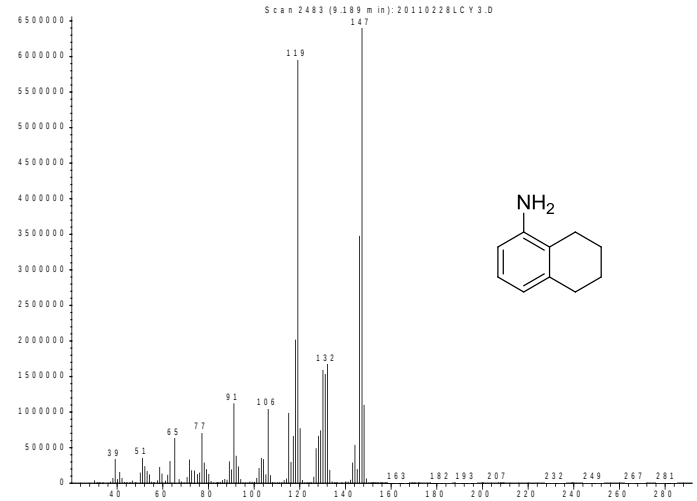

Fig. S23 Mass spectra of 5,6,7,8-tetrahydronaphthalen-1-amine

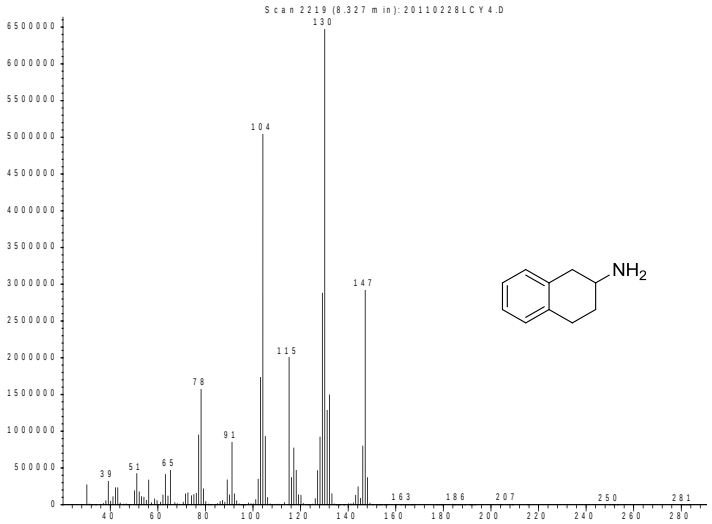

Fig. S24 Mass spectra of 1,2,3,4-tetrahydronaphthalen-2-amine

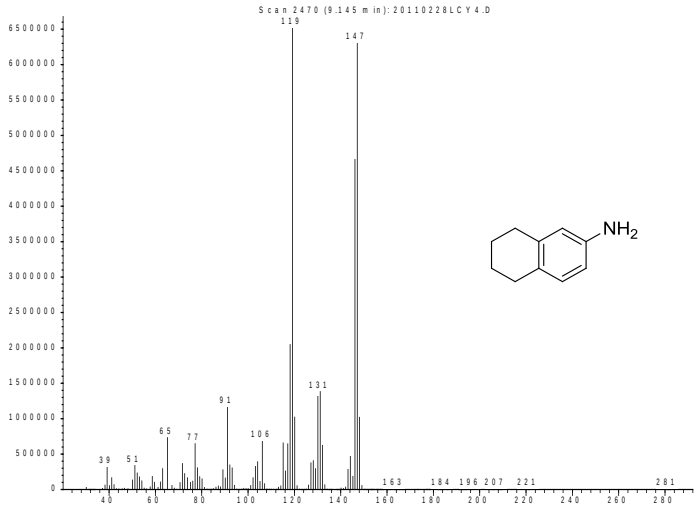

Fig. S25 Mass spectra of 5,6,7,8-tetrahydronaphthalen-2-amine

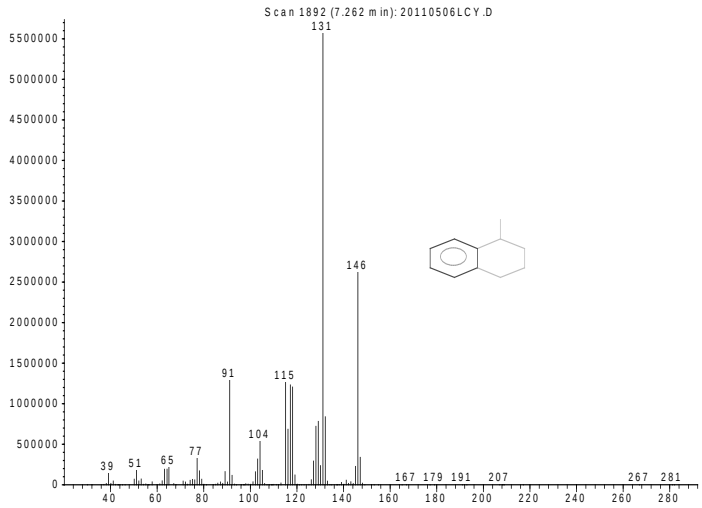

Fig. S26 Mass spectra of 1-methyl-1,2,3,4-tetrahydronaphthalene

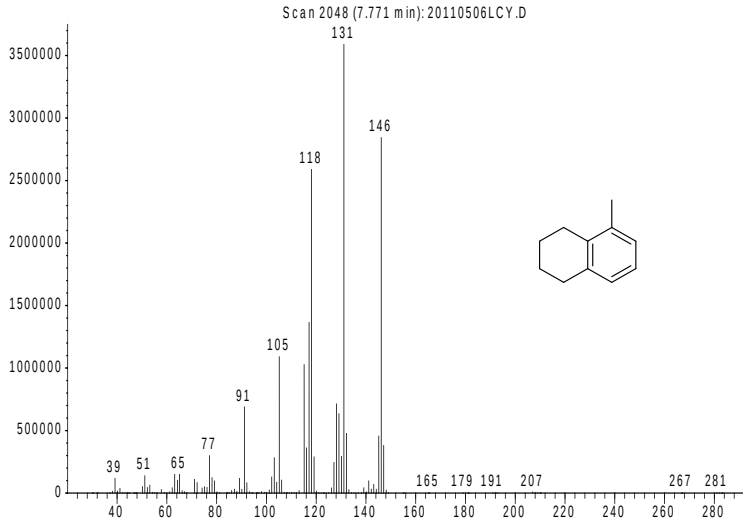

Fig. S27 Mass spectra of 5-methyl-1,2,3,4-tetrahydronaphthalene

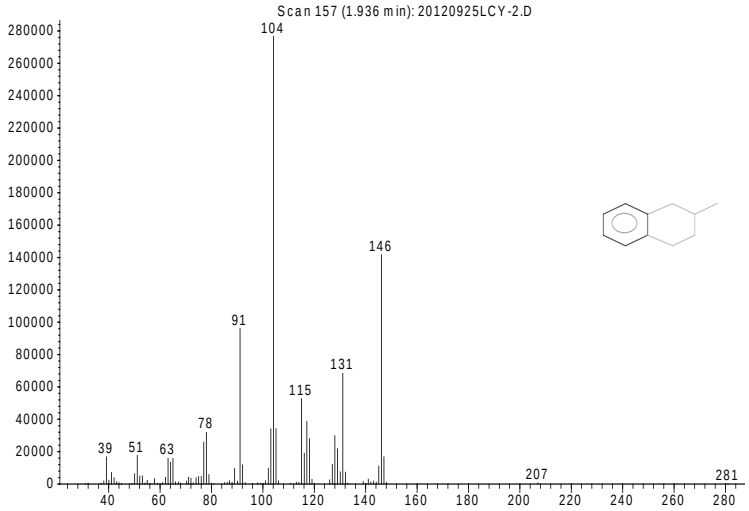

Fig. S28 Mass spectra of 2-methyl-1,2,3,4-tetrahydronaphthalene

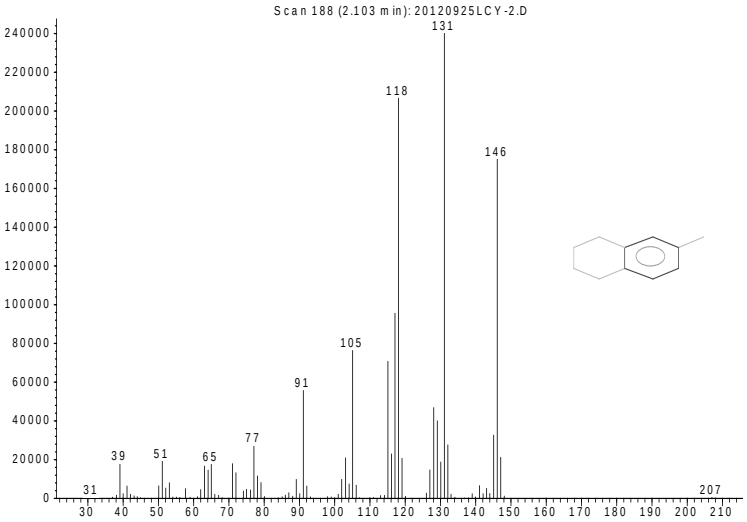

Fig. S29 Mass spectra of 6-methyl-1,2,3,4-tetrahydronaphthalene

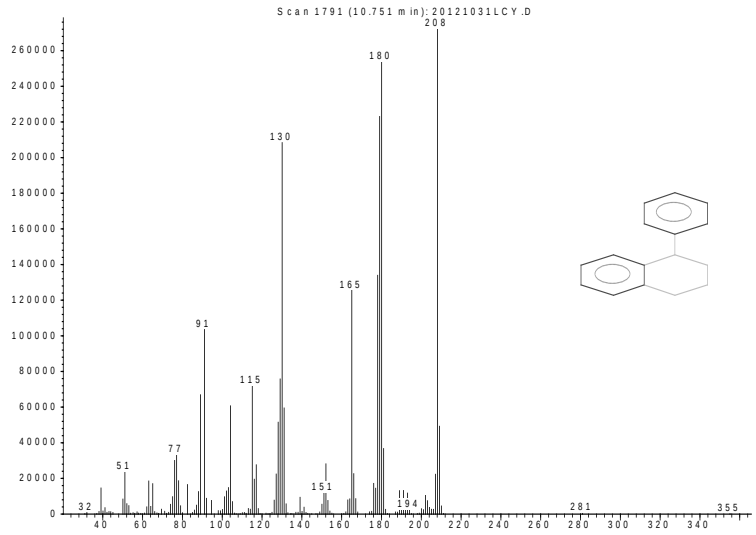

Fig. S30 Mass spectra of 1-phenyl-1,2,3,4-tetrahydronaphthalene

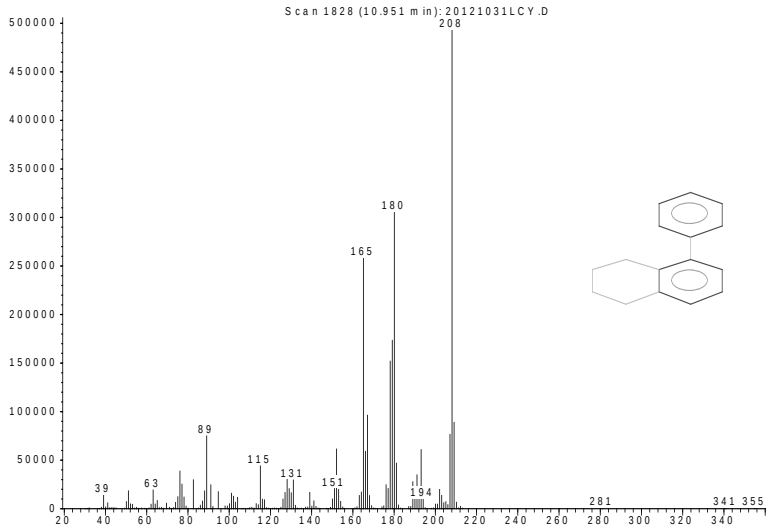

Fig. S31 Mass spectra of 5-phenyl-1,2,3,4-tetrahydronaphthalene

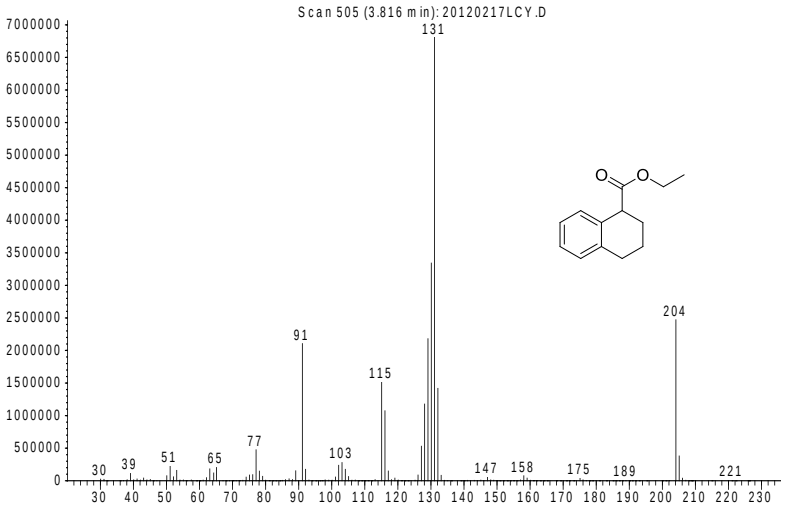

Fig. S32 Mass spectra of ethyl 1,2,3,4-tetrahydronaphthalene-1-carboxylate

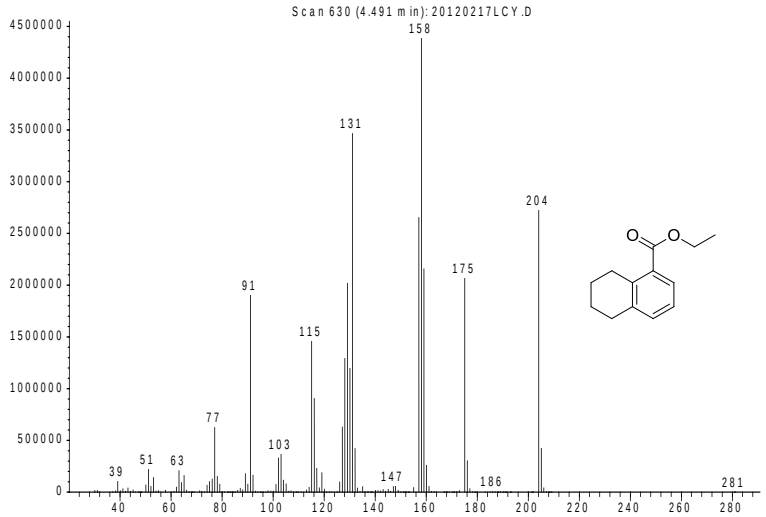

Fig. S33 Mass spectra of ethyl 5,6,7,8-tetrahydronaphthalene-1-carboxylate

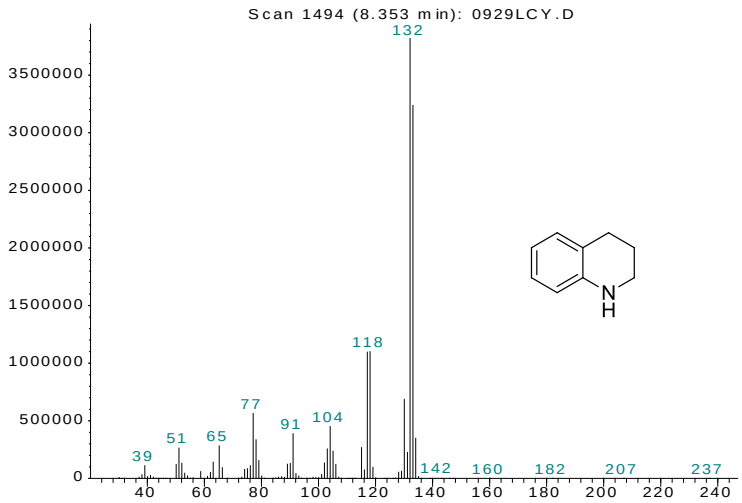

Fig. S34 Mass spectra of 1,2,3,4-tetrahydroquinoline

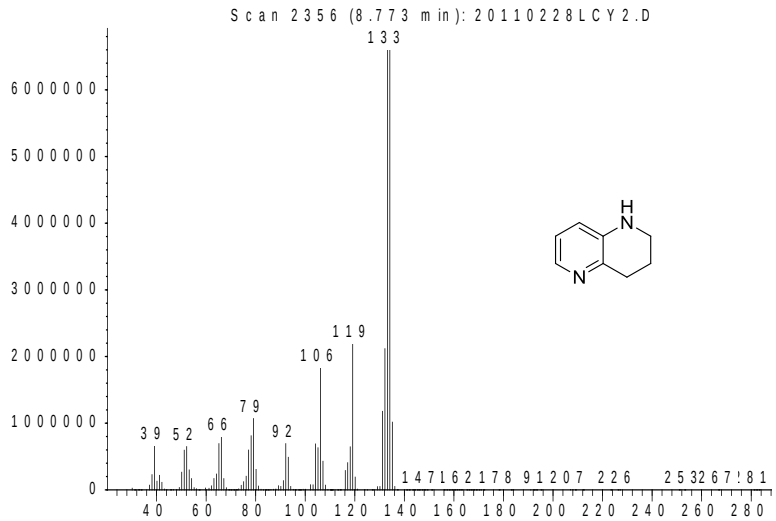

Fig. S35 Mass spectra of 1,2,3,4-tetrahydro-1,5-naphthyridine

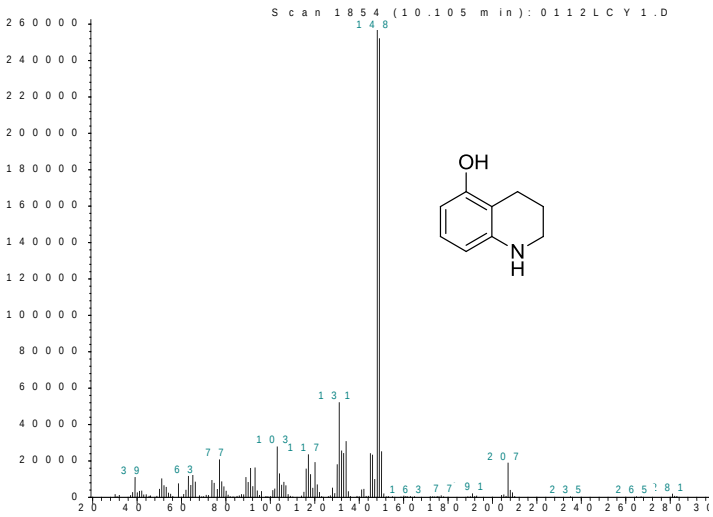

Fig. S36 Mass spectra for 1,2,3,4-8-tetrahydroquinolinol

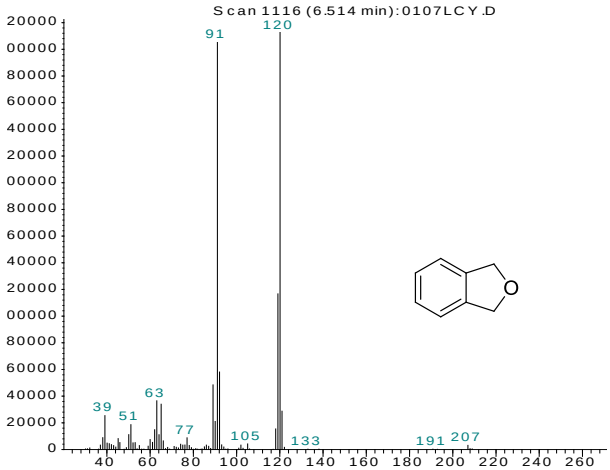

Fig. S37 Mass spectra of 1,3-dihydroisobenzofuran

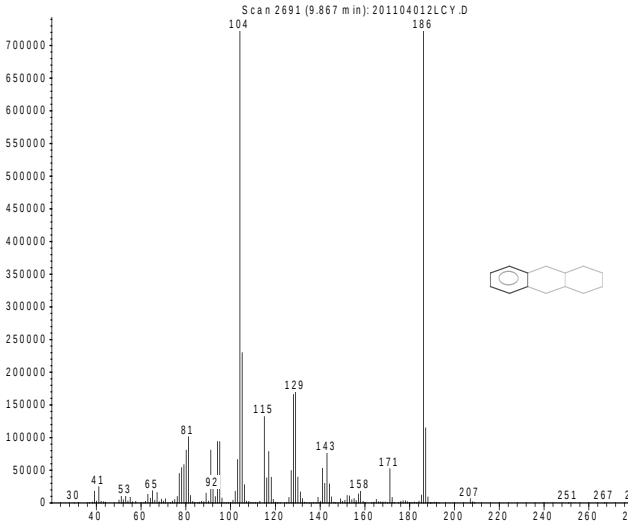

Fig. S38 Mass spectra of 1,2,3,4,4a,9,9a,10-octahydroanthracene

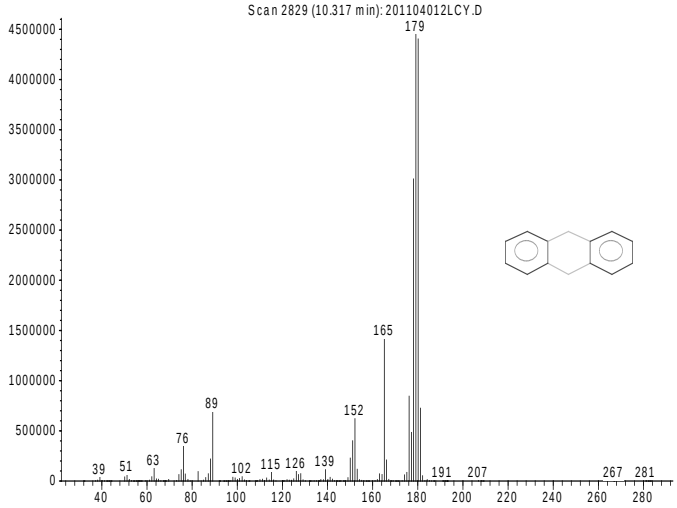

Fig. S39 Mass spectra of 9,10-dihydroanthracene

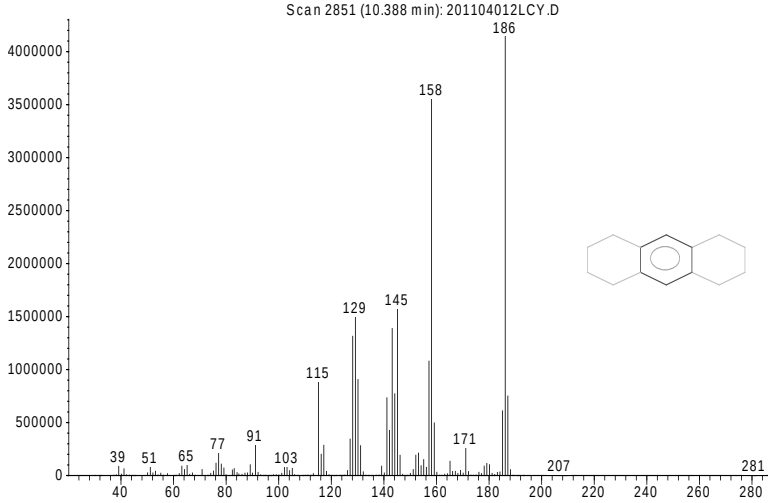

Fig. S40 Mass spectra of 1,2,3,4,5,6,7,8-octahydroanthracene

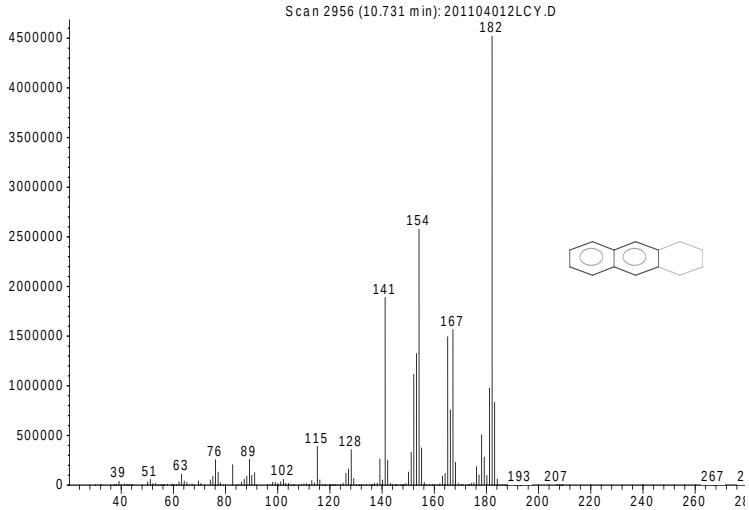

Fig. S41 Mass spectra of 1,2,3,4-tetrahydroanthracene

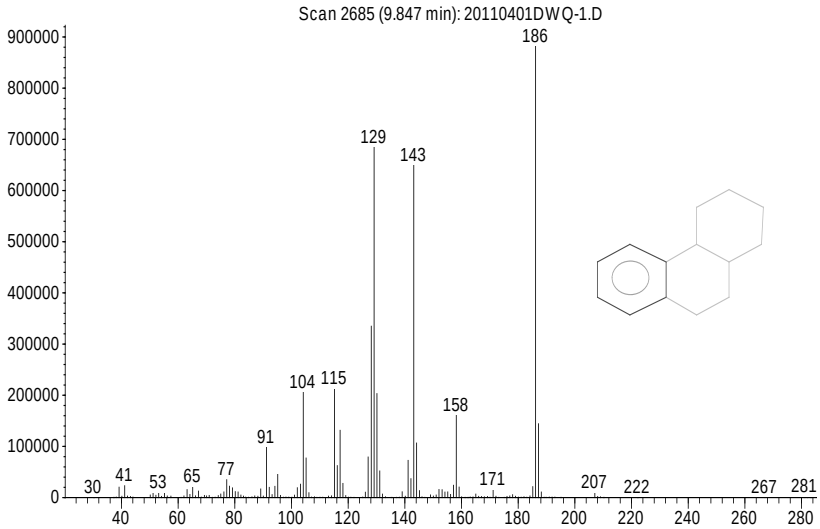

Fig. S42 Mass spectra of 1,2,3,4,4a,9,10,10a-octahydrophenanthrene

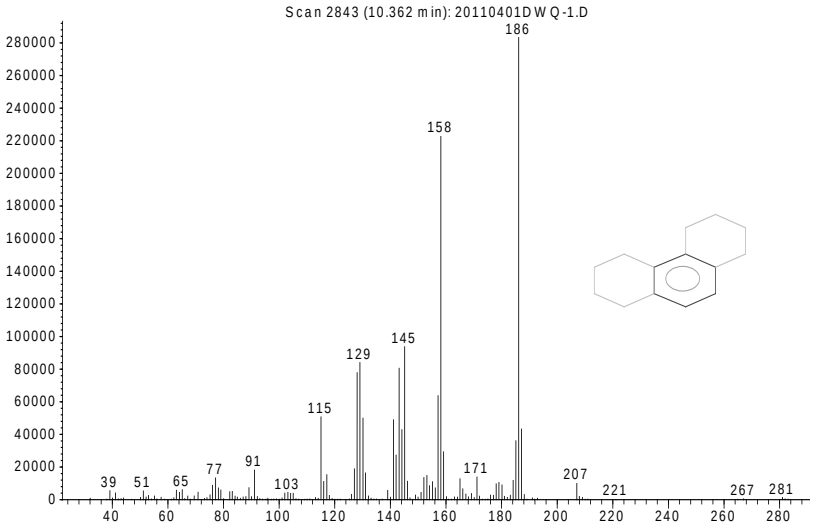

Fig. S43 Mass spectra of 1,2,3,4,5,6,7,8-octahydrophenanthrene

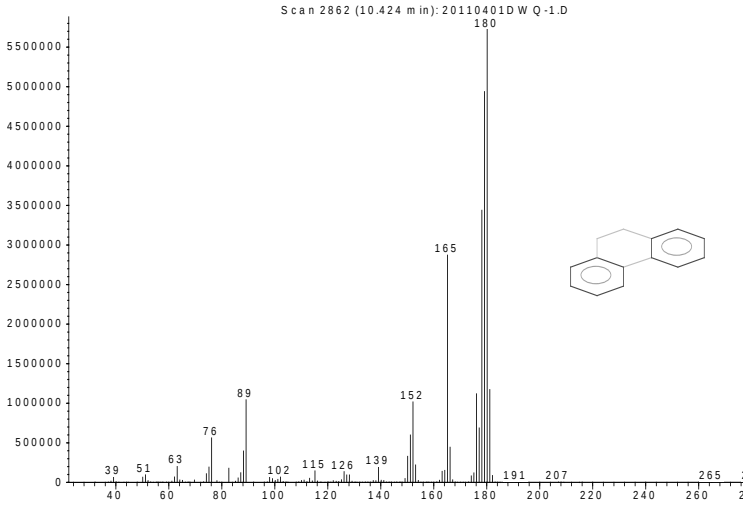

Fig. S44 Mass spectra of 9,10-dihydrophenanthrene

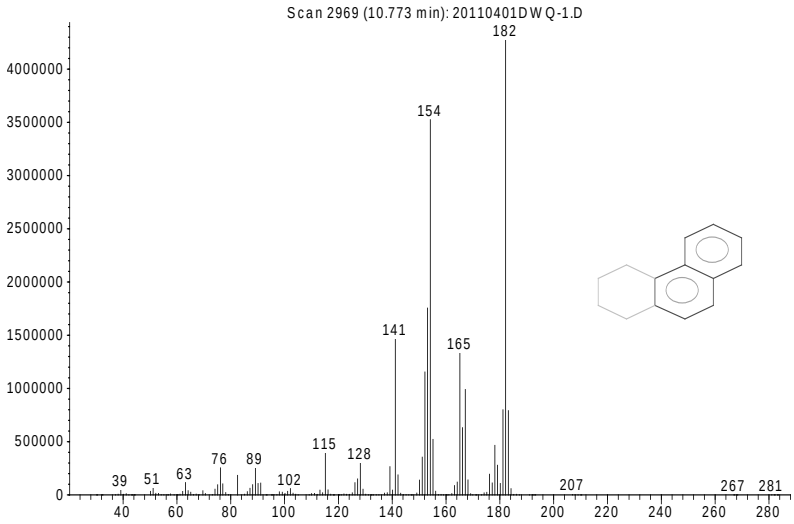

Fig. S45 Mass spectra of 1,2,3,4-tetrahydrophenanthrene

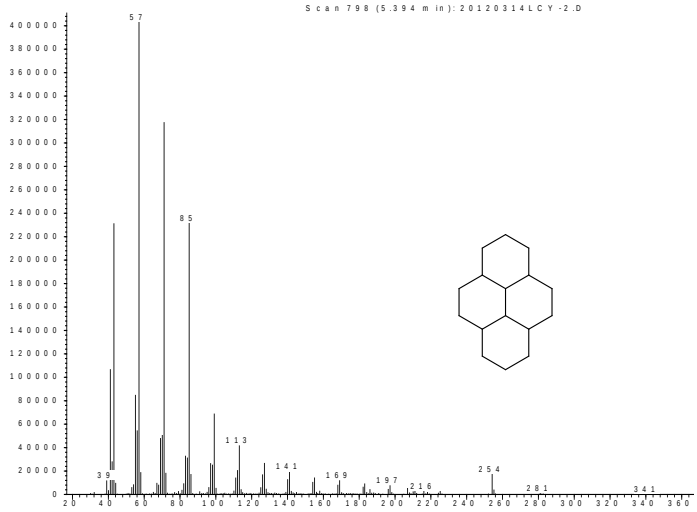

Fig. S46 Mass spectra of hexadecahydropyrene

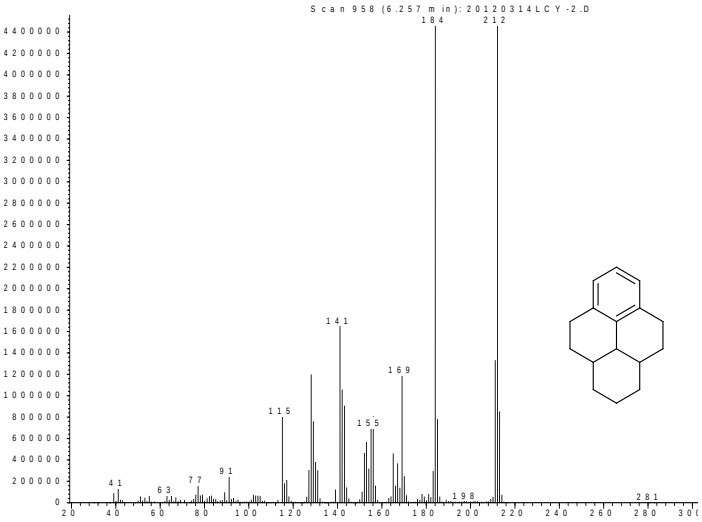

Fig. S47 Mass spectra of 1,2,3,3a,3a1,4,5,9,10,10a-decahydropyrene

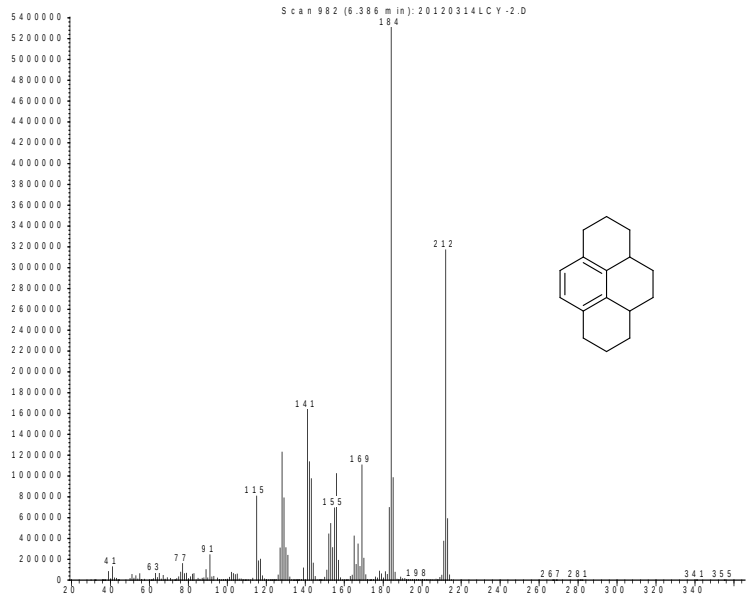

Fig. S48 Mass spectra of 1,2,3,3a,4,5,5a,6,7,8-decahydropyrene

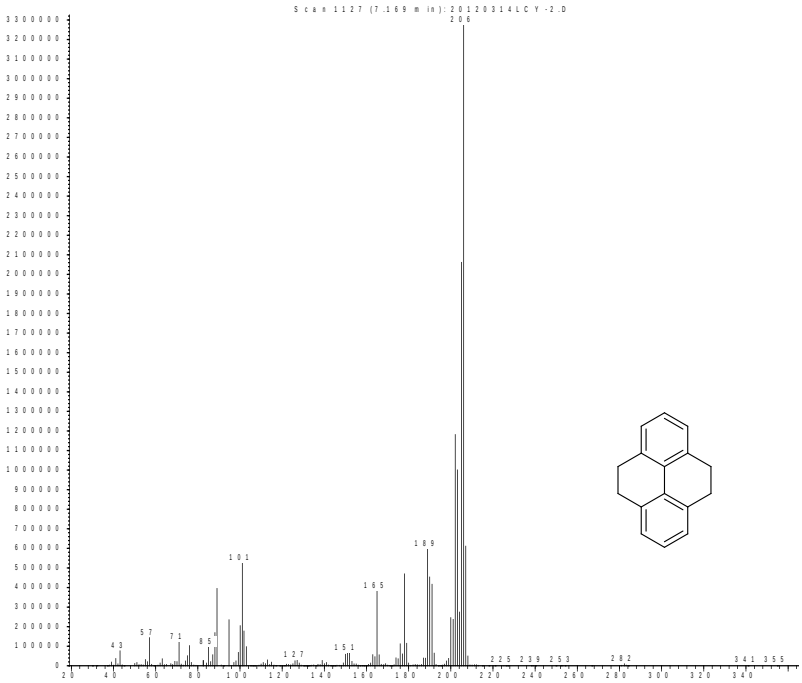

Fig. S49 Mass spectra of 4,5,9,10-tetrahydropyrene

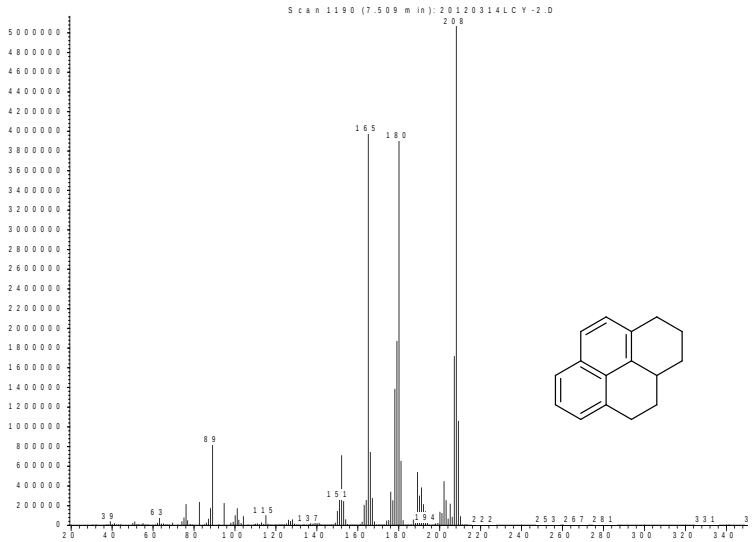

Fig. S50 Mass spectra of 1,2,3,3a,4,5-hexahydropyrene

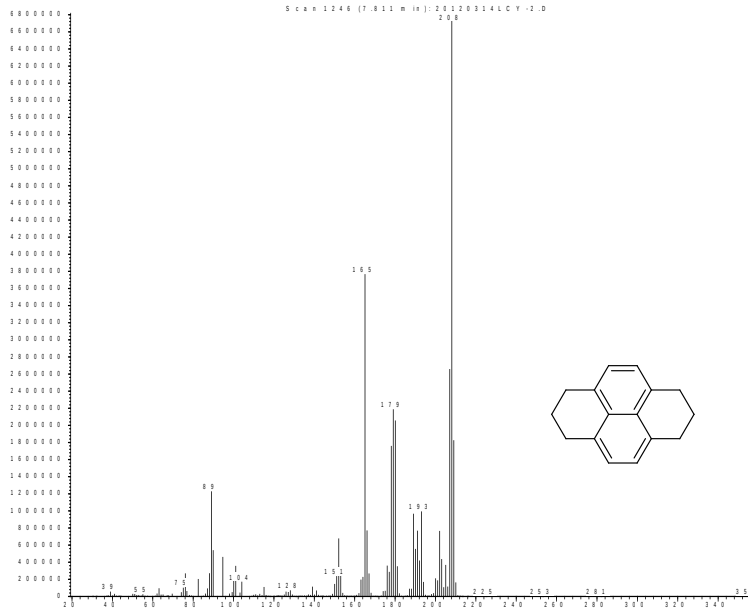

Fig. S51 Mass spectra of 1,2,3,6,7,8-hexahydropyrene

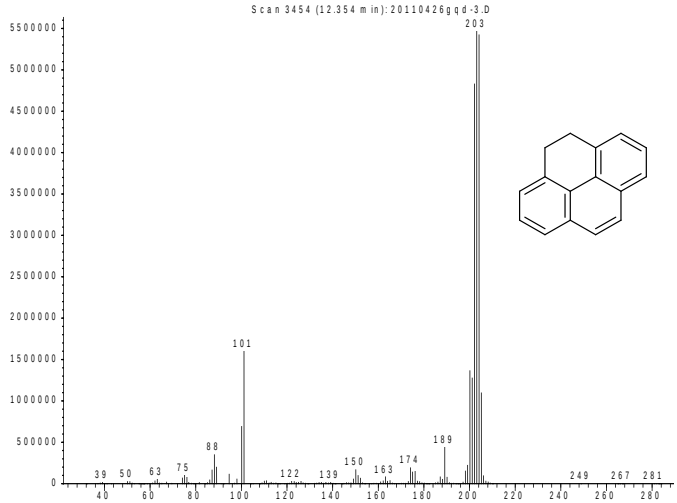

Fig. S52 Mass spectra of 4,5-dihydropyrene

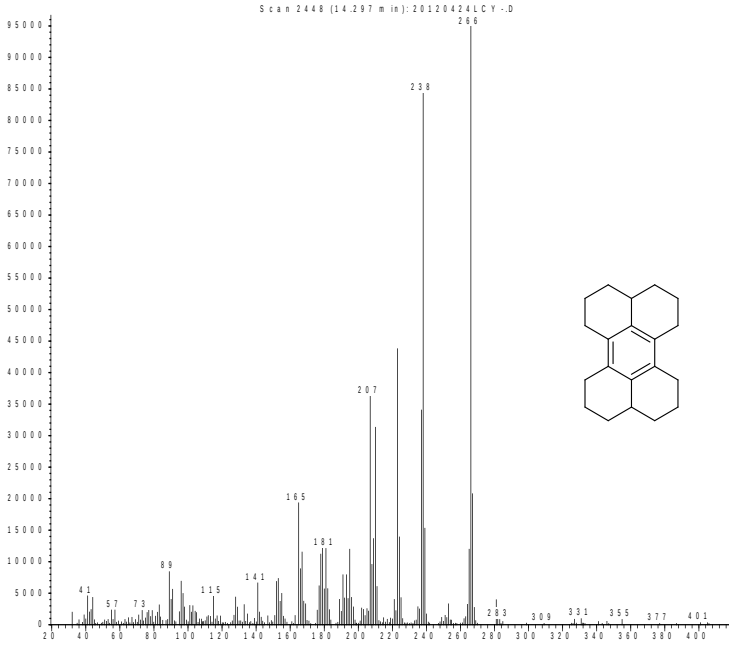

Fig. S53 Mass spectra of 1,2,3,3a,4,5,6,7,8,9,9a,10,11,12-tetradecahydroperylene

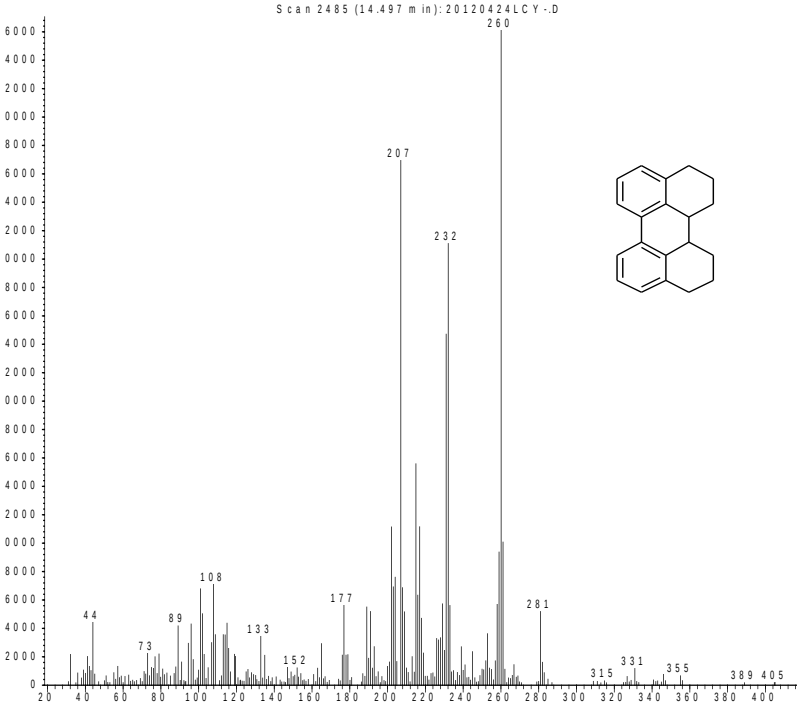

Fig. S54 Mass spectra of 1,2,3,10,11,12,12a,12b-octahydroperylene

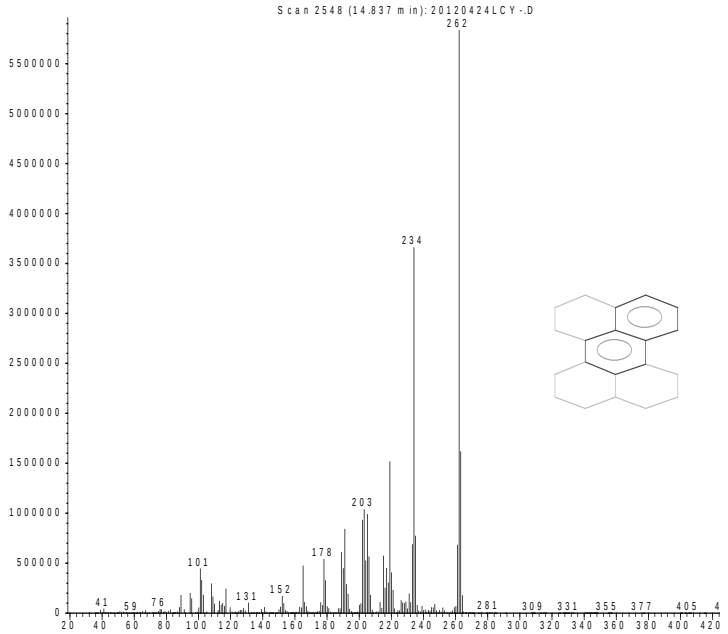

Fig. S55 Mass spectra of 1,2,3,3a,4,5,6,7,8,9-decahydroperylene

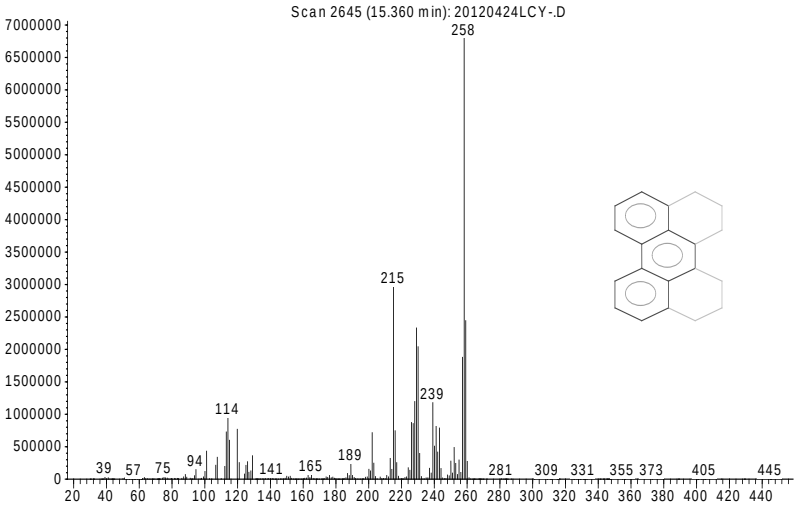

Fig. S56 Mass spectra of 1,2,3,10,11,12-hexahydroperylene

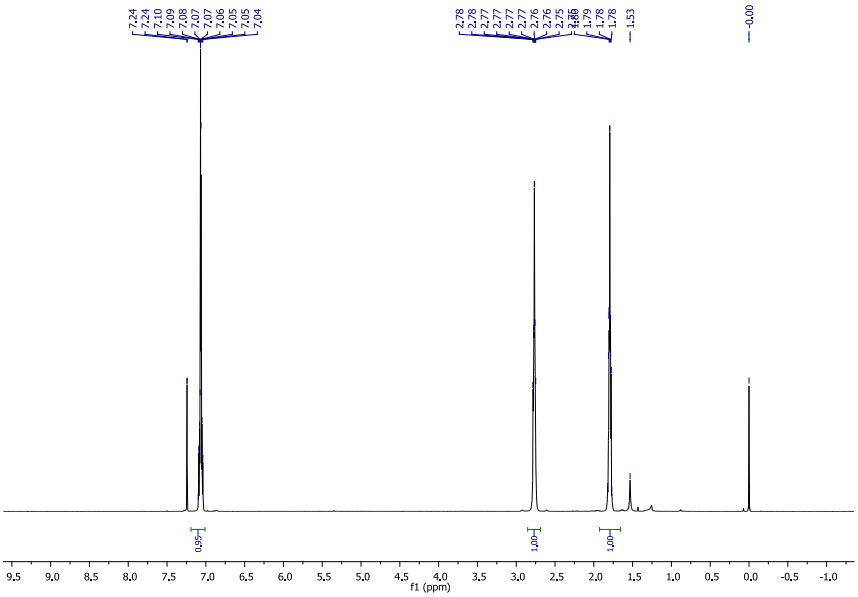

Fig. S57 ^{1}H NMR spectrum of tetralin

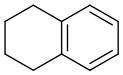

^{1}H NMR (400 MHz, $CDCl_3$): δ =1.78-1.79 (m,4H), 2.75-2.78 (m,4H), 7.04-7.24(m,4H)

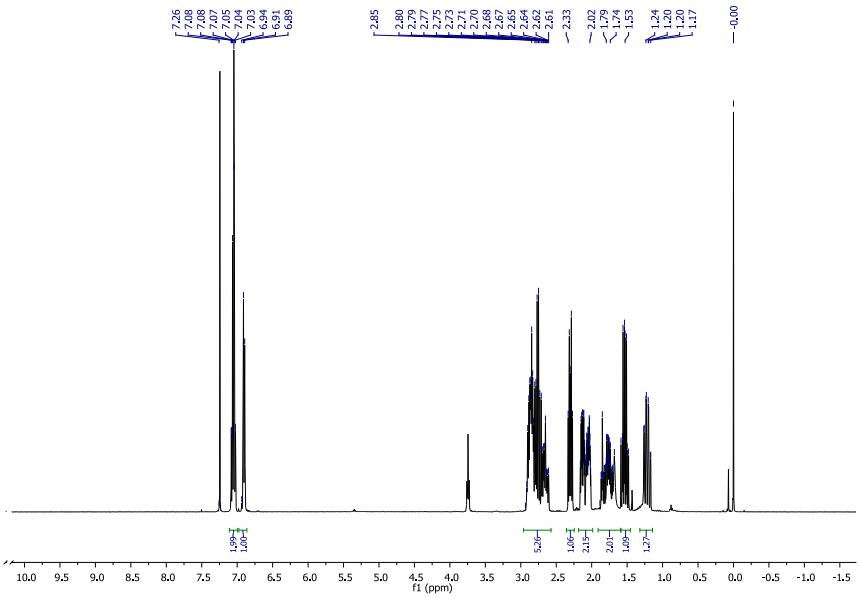

Fig. S58 ^{1}H NMR spectrum of 1,2,2a,3,4,5-hexahydroacenaphthylene

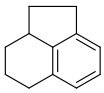

^{1}H NMR (400 MHz, $CDCl_3$): δ =1.17-1.24 (m,1H), 1.48-1.59 (m,1H), 1.72-1.85 (m,2H), 2.01-2.14 (m,2H), 2.27-2.33 (m,1H), 2.61-2.93 (m,5H), 6.89-6.94 (m,1H), 7.03-7.07 (m,2H).

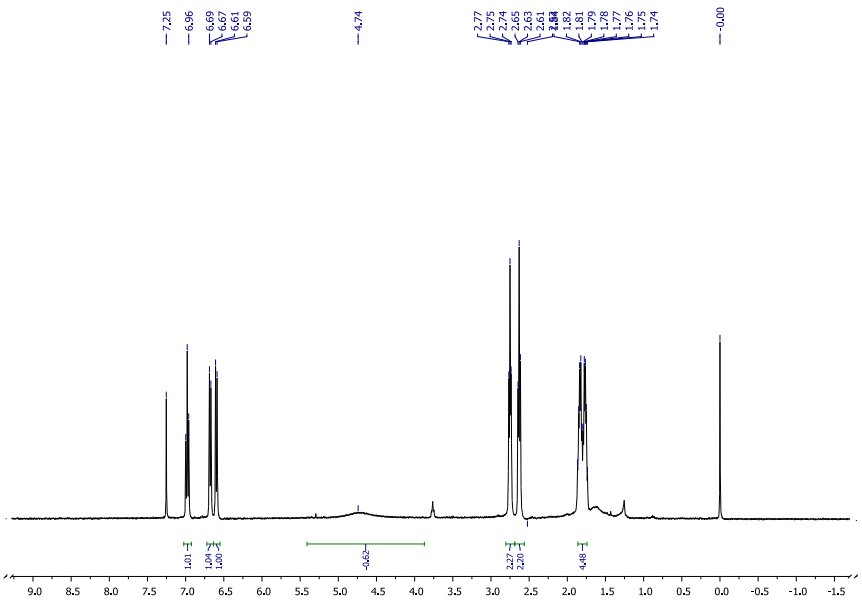

Fig. S59 ^{1}H NMR spectrum of 5,6,7,8-tetrahydronaphthalen-1-ol

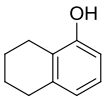

^{1}H NMR (400 MHz, $CDCl_3$): δ =1.74-1.87 (m, 4H), 2.61-2.65 (t,2H), 2.74-2.77 (t,2H), 4.74 (s,-OH, 1H), 6.9-6.61 (d, *J*=8Hz, 1H), 6.67-6.69 (d, *J*=8Hz, 1H), 6.96-7.00 (t,1H).

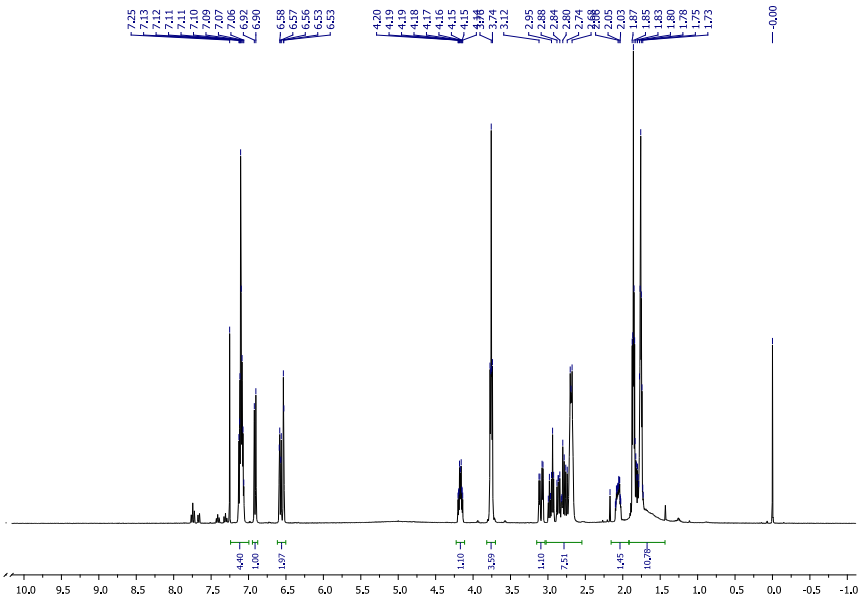

Fig. S60 ^{1}H NMR spectrum of the mixture of hydrogenatd naphthalen-2-ol

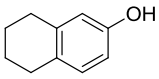

5,6,7,8-tetrahydronaphthalen-2-ol (A)

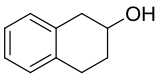

1,2,3,4-tetrahydronaphthalen-2-ol (B)

^{1}H NMR (400 MHz, $CDCl_3$): δ =6.53-6.59 (m, 3H) stands for the protons of benzenoid rings of A. δ =6.90-6.92 (d, *J*=8Hz, 2H) and δ =7.06-7.25 (m, 2H) stand for the protons of benzenoid rings of B. Therefore, the ration between the A and B can be calcualted by n(A)/n(B)=0.73which is similar to the results detected by GC.

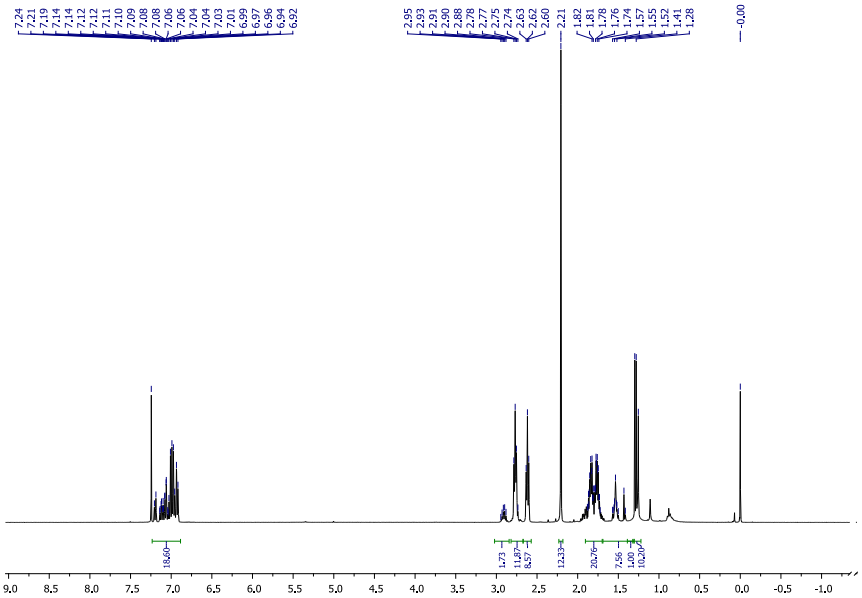

Fig. S61 ^{1}H NMR spectrum of the mixture of hydrogenated 1-methyl-naphthalene

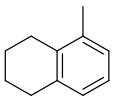

5-methyl-1,2,3,4-tetrahydronaphthalene (A)

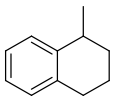

1-methyl-1,2,3,4-tetrahydronaphthalene (B)

^{1}H NMR (400 MHz, $CDCl_3$): δ =1.25-1.30 (m, -CH_3, 3H) and δ =2.21 (s, -CH_3, 3H) stand for the protons of methyl of B and A. Therefore, the ration between the A and B can be calcualted by n(A)/n(B)=12.33/10.20=1.21which is similar to the results detected by GC.

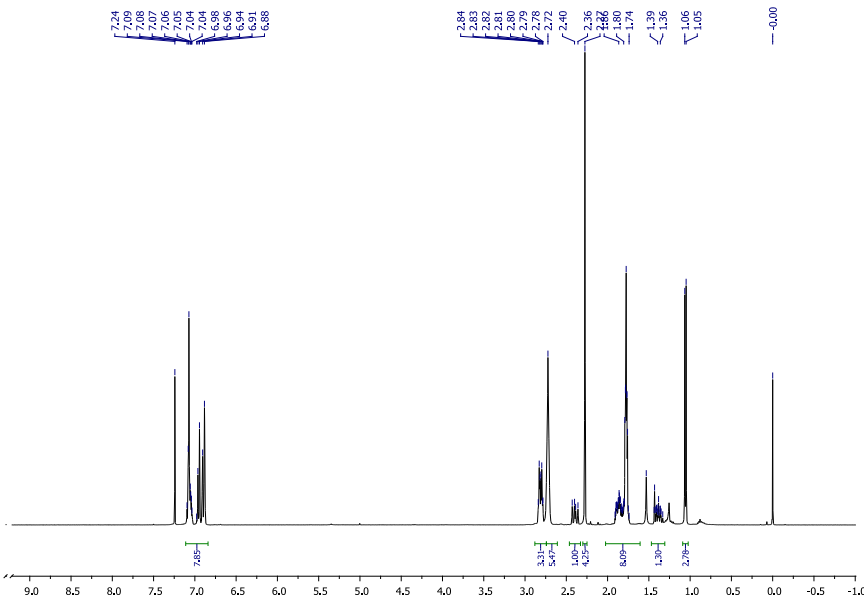

Fig. S62 ^{1}H NMR spectrum of the mixture of hydrogenated 2-methylnaphthalene

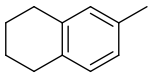

6-methyl-1,2,3,4-tetrahydronaphthalene (A)

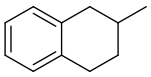

2-methyl-1,2,3,4-tetrahydronaphthalene (B)

^{1}H NMR (400 MHz, $CDCl_3$): δ =1.05-1.06 (d, J=4Hz, -CH_3, 3H) and δ =2.275 (s, -CH_3, 3H) stand for the protons of methyl of B and A. Therefore, the ration between the A and B can be calcualted by n(A)/n(B)=4.25/2.78=1.53 which is similar to the results detected by GC.

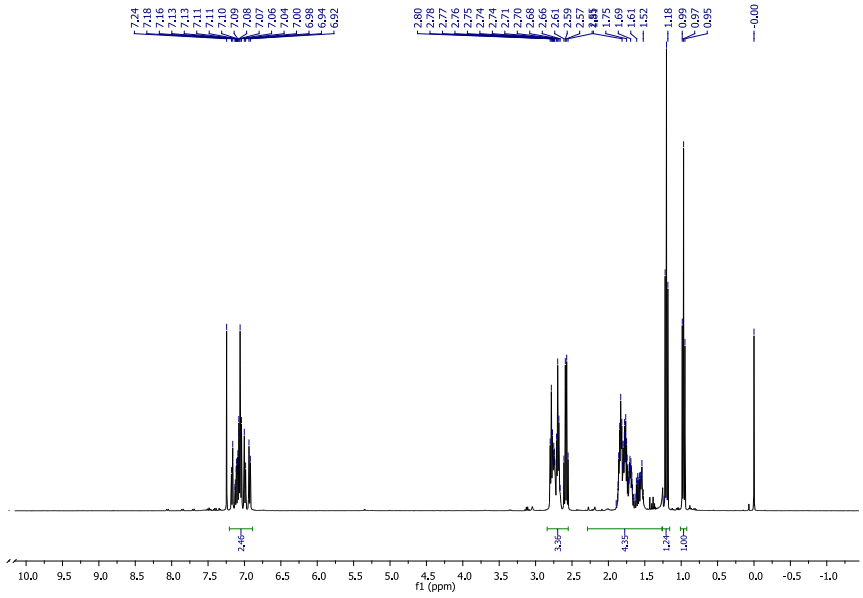

Fig. S63 ^{1}H NMR spectrum of the mixture of hydrogenated 1-ethylnaphthalene

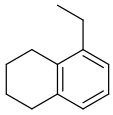

5-ethyl-1,2,3,4-tetrahydronaphthalene (A)

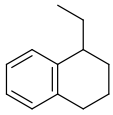

1-ethyl-1,2,3,4-tetrahydronaphthalene (B)

^{1}H NMR (400 MHz, $CDCl_3$): δ =0.95-0.99 (t,3H), 1.18-1.21 (t,3H).

The protons at δ =0.95-0.99 (t,3H), 1.18-1.21 (t,3H) reprent the protons of methyls in the molecular A and B, repectively. So, the ration between A and B can be calculated as n(A)/n(B)=1.24/1.00=1.24 which is similar to the results detected by GC.

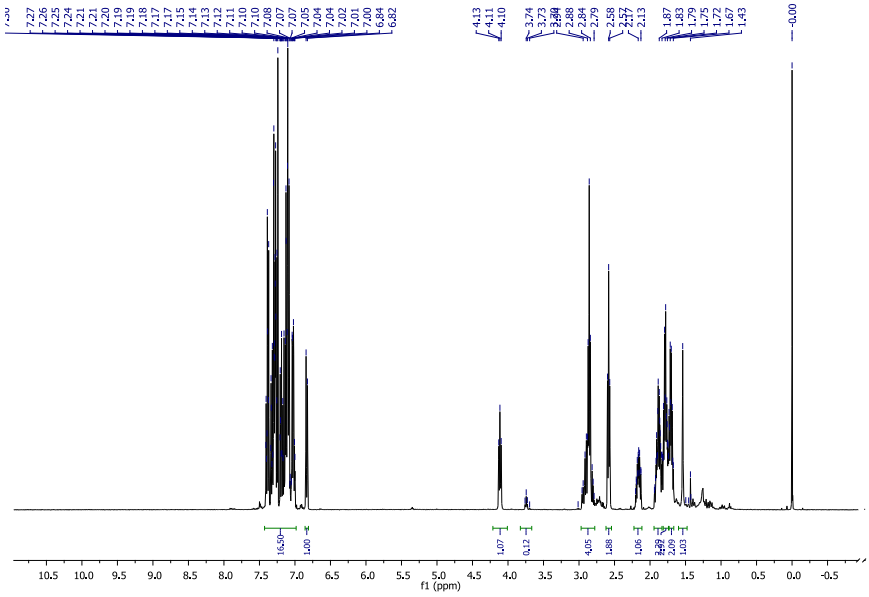

Fig. S64 ^{1}H NMR spectrum of the mixture of hydrogenated 1-phenylnaphthalene

^{1}H NMR (400 MHz, $CDCl_3$): δ = 4.10-4.13 (t, 1H), 6.82-7.30 (m, 18H). The proton at the δ = 4.10-4.13 stands for the Ha in the molecular of 1-phenyl-1,2,3,4-tetrahydronaphthalene. And the

protons within the ranges of δ =6.82-7.30 stand for the protons of benzen rings in the molecuar of hydrogeanted 1-phenylnaphthalene.

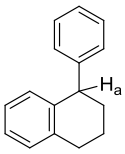

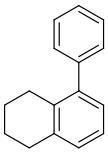

1-phenyl-1,2,3,4-tetrahydronaphthalene (A) 5-phenyl-1,2,3,4-tetrahydronaphthalene(B)

Because in the molecular of 1-phenyl-1,2,3,4-tetrahydronaphthalene, the protons of benzen rings are 9 times of the number of Ha. So the ratio between n(A)/n(B)=(9×1.07)/(17.5-9×1.07)=1.22 which is similar to the results detected by GC.

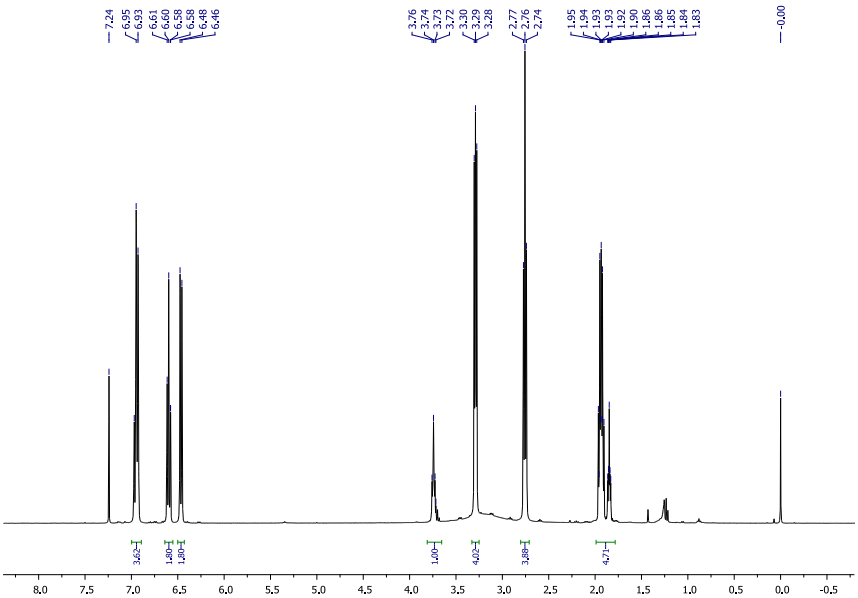

Fig. S65 ^{1}H NMR spectrum of 1,2,3,4-tetrahydroquinoline

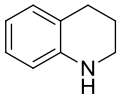

^{1}H NMR (400 MHz, $CDCl_3$): δ =1.83-1.95 (m, 2H), 2.74-2.77 (t, 2H), 3.28-3.30 (t,2H), 3.72-3.76 (m,1H, -NH), 6.46-6.48 (d, *J*=8Hz, 1H), 6.58-6.61 (t,1H), 6.93-6.95 (d, *J*=8Hz, 1H).

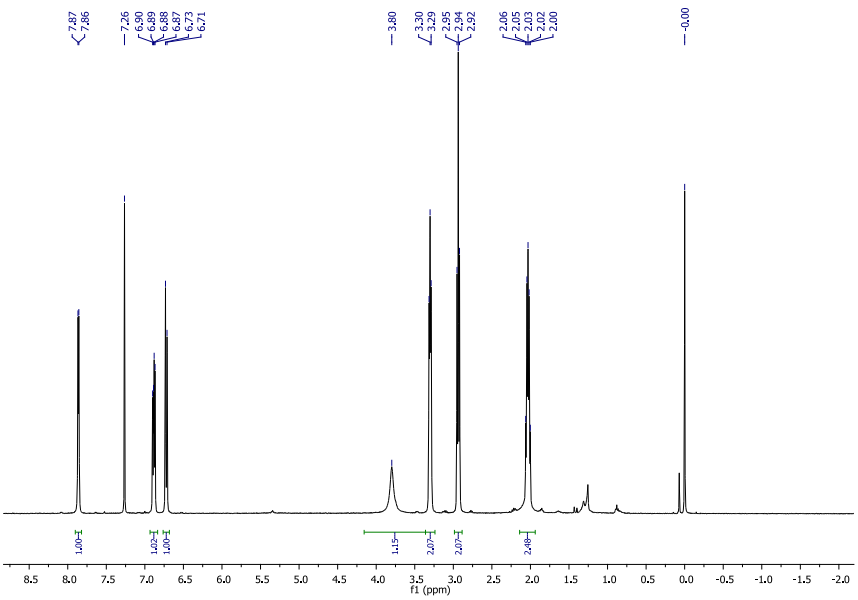

Fig. S66 ^{1}H NMR spectrum of 1,2,3,4-tetrahydro-1,5-naphthyridine

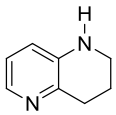

^{1}H NMR (400 MHz, $CDCl_3$): δ =2.00-2.06 (m,2H), 2.92-2.95 (t,2H), 3.29-3.30 (t, 2H), 3.80 (s,1H,-NH), 6.71-6.73 (d,*J*=8Hz,1H), 6.87-6.90 (m,1H), 7.86-7.87 (d, *J*=4Hz,1H)

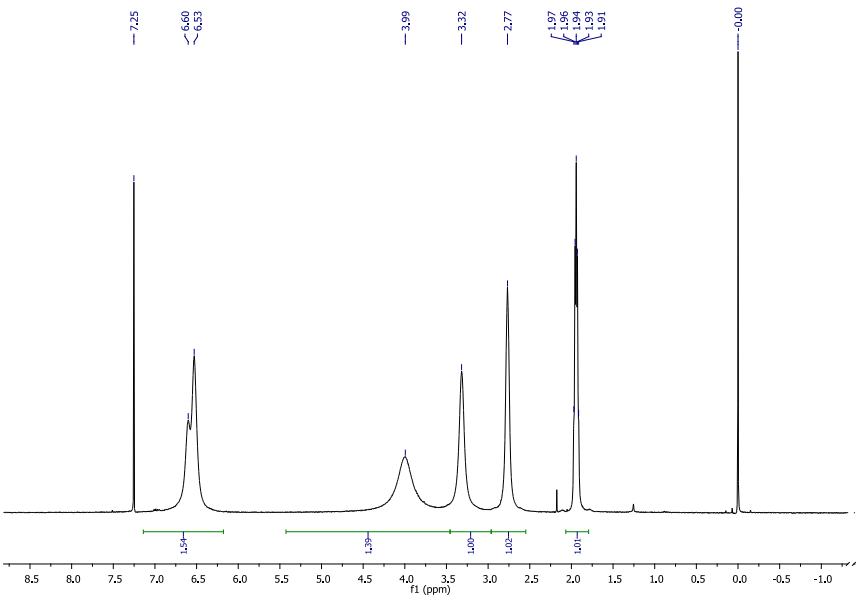

Fig. S67 ^{1}H NMR spectrum of 1,2,3,4-tetrahydroquinolin-5-ol

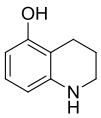

^{1}H NMR (400 MHz, $CDCl_3$): δ =1.91-1.97 (m, 2H), 2.77 (s,2H), 3.32 (s, 2H), 3.99 (m,2H), 6.53-6.60 (d, J=28Hz, 3H)

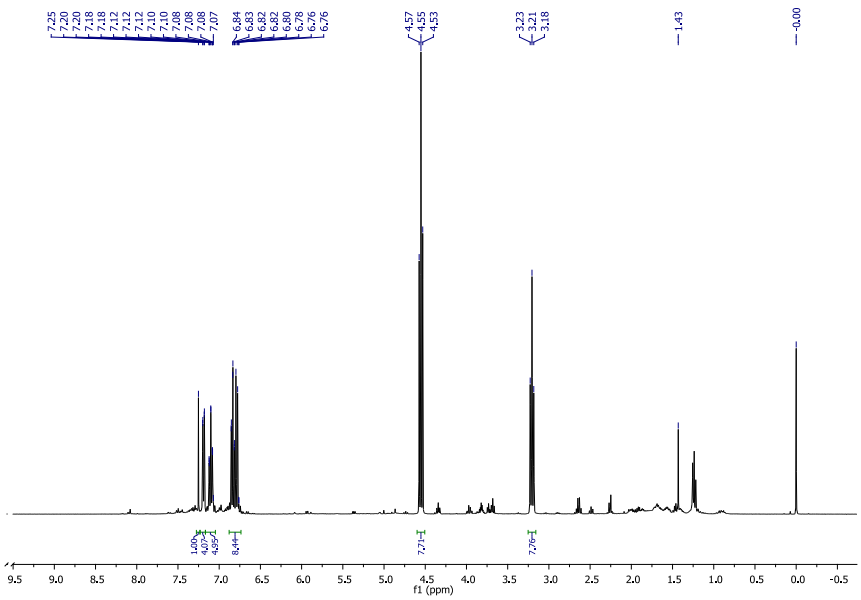

Fig. S68 ^{1}H NMR spectrum of 2,3-dihydrobenzofuran

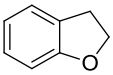

^{1}H NMR (400 MHz, $CDCl_3$): δ =3.18-3.23(t, 2H), 4.53-4.57(t,2H), 6.76-7.25(m, 4H)